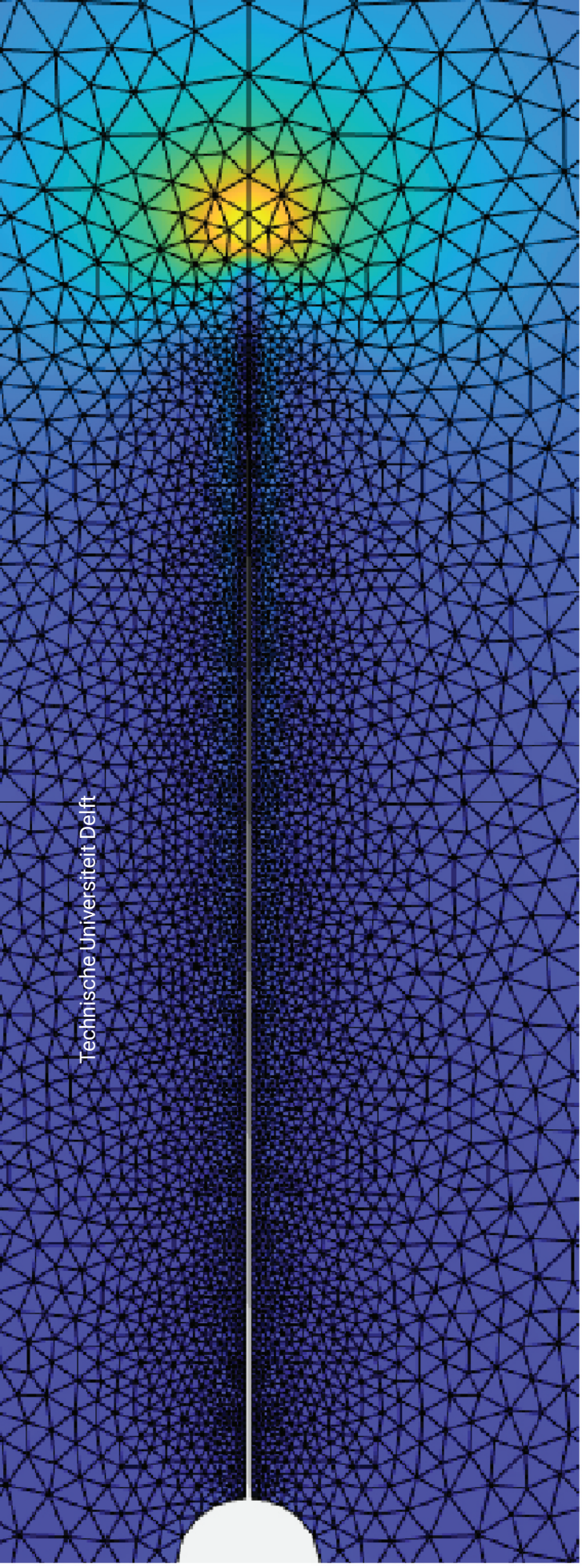

A stiffness independent Interfacial Thick Level Set method

A modified approach for crack analysis

Joep Sluijs

TU Delft

A stiffness independent Interfacial Thick Level Set method

A modified approach for crack analysis

by

Joep Sluijs

to obtain the degree of Master of Science in Structural Engineering
at the Delft University of Technology,
to be defended publicly on Friday July 17th, 2020 at 12:00 PM.

Student number:	4245865	
Project duration:	October, 2019 – July, 2020	
Thesis committee:	Dr. ir. F. P. van der Meer,	TU Delft, chair
	Ir. R. Dekker,	TU Delft, daily supervisor
	Dr. ir. M. Pavlovic,	TU Delft

An electronic version of this thesis is available at `http://repository.tudelft.nl/`.

TU Delft

Preface

For the past 9 months I have worked on my Master Thesis project. The document you are now reading is the result of this work. For me it also represents the end of an amazing time, some would even say a long time, as a student at the Delft University of Technology. Hopefully it will also be the beginning of great new adventures and opportunities. I am very grateful for everything that I have learned and experienced by walking around the faculty of Civil Engineering for the past 8 years.

During my research I have learned a lot about the damage mechanics and fracture mechanics regarding crack growth. Furthermore, I have learned a lot about numerical modeling and working on such an extensive research. Personally, this time was very valuable and I'm grateful for the given opportunity to do a research containing so much elements that are of interest to me.

First of all I would like to thank Frans van der Meer for offering me the opportunity to do a research that enabled me to work with a lot of subjects that have my interest, such as numerical modeling and learning to use new programming languages. Most of all I would like to thank Frans for his constructive feedback during our meetings every two weeks and his willingness to answer all my questions. I would also like to thank Richard Dekker, who was my daily supervisor during this process. If I had any problems with my research I could always knock on his door, or later the digital door of course, and he would be ready to help me out. It meant a lot to me and helped me a great amount in periods that I was not sure how to proceed with this research. Furthermore, I would like to thank Marko Pavlocic for his feedback on my work and by challenging me to see this numerical research in a more real and physical way.

Then I would like to acknowledge and thank some individuals that helped me a lot during this period. First of all I would like to thank my girlfriend Emma Kolk who supported me throughout the whole process and who picked me up whenever I had trouble to stay motivated. Furthermore, she helped me with the graphics that you, the reader, can see in this document. I would also like to thank Tessa Rombouts and Yanniek Vallenduuk for being my study buddies, which made working on my Thesis a lot more fun.

At last, I would like to thank my family and friends for their support and motivation throughout the last 9 months.

Joep Sluijs
Delft, July 2020

Abstract

Crack growth is an important failure mechanism in many engineering materials. Numerical models for crack growth have been developed within the framework of damage mechanics. All these models aim for the same goal, obtaining accurate results for crack growth under various loading conditions. Many damage models are based upon the cohesive crack approach. However, level set based models provide advantages compared to the cohesive crack models with regard to fatigue analysis. Latifi et al. [9] proposed an alternative method to the existing thick level set (TLS) method, the interfacial thick level set (ITLS) model. The use of interface elements made the model more suitable to simulate several failure processes. In this thesis it is demonstrated that this method suffers from a dependency on the initial interfacial stiffness for the global response of a system by conducting a parameter study under quasi-static loading conditions. All interfacial parameters, which include damage shape parameters, damage length and initial stiffness, that are of interest for the ITLS model are investigated, to measure the individual influence of each parameter on the global response. This parameter study proves that for a varying value of the initial interfacial stiffness parameter K the global response varies as well. This gives motivation to conduct further research on the removal of the initial interfacial stiffness from the current ITLS model.

Two methods are developed to overcome this initial interfacial stiffness dependency. The first method assumes that the initial interfacial stiffness dependency is caused by the current formulation of the constitutive law of the interface. A new expression for the interfacial stiffness is adapted after which all constitutive relations are updated. Due to the adapted formulation for the interfacial stiffness, the bounds for the damage function also have to be adapted resulting in the addition of a lower bound l_{bound}. The new method shows a perfect agreement with the current ITLS model, which validates the method as an accurate alternative. Compared to the current ITLS model, method 1 allows for the control of the initial stiffness of the undamaged part of the interface by changing l_{bound} without affecting the global response. However, when executing simulations for a varying initial interfacial stiffness K the same problem as for the current ITLS is observed. It can be concluded that in a way this method removes the dependency on the initial interfacial stiffness but the initial interfacial stiffness parameter K should then remain constant. Furthermore, the calibration process is not simplified compared to the current ITLS model. For this reason method 1 is rejected as the final solution to the problem and a second method is proposed.

The second method assumes a direct relation between the damage parameter c_1 and the initial interfacial stiffness parameter K. This damage parameter is responsible for the steepness of the damage profile. The results from the parameter study showed that an increase of one of these parameters results in opposite behaviour for the initial stiffness of the global response. The leading hypothesis becomes that an increase in the stiffness parameter K can be neutralized by an increase in the damage parameter c_1. Proportionality between both parameters is assumed. By trial and error the proportionality is found to be one to one. When using this proportionality condition, simulations with different values for the initial interfacial stiffness showed a perfect agreement for the load-displacement and the crack growth responses. Moreover, the proportionality condition is accurate for both a linear elastic (LE) material and an elastic-plastic (EP) material. The proportionality condition is proven by elaborating the interfacial stiffness over the damaged zone. This elaboration is done both numerically and analytically and proves that there is a one to one proportionality between c_1 and K, which validates the replacement of c_1 by a constant c multiplied with K. Lastly, the method should be compared to a response obtained through a different type of analysis. The method is compared with the solution of an analytical analysis resulting in a very good agreement for both a LE and an EP material. Therefore, method 2 can be approved as a solution to the initial interfacial stiffness dependency problem.

The adapted ITLS model following method 2 with the proportionality condition is proven to be accurate and robust for simulations with a quasi-static loading type. A study on fatigue loading with the adapted ITLS was also carried out. For the adapted model to be valid, the amount of plasticity and the computed variation of energy release rate should be independent of the choice for the initial interfacial stiffness K. The results show that such behaviour is obtained for a compact-tension test. Therefore, the adapted ITLS model seems to be accurate for simulating crack growth under fatigue loading. However, further research on the ITLS model for fatigue is necessary in order to propose the adapted ITLS model as the new approach for crack growth simulation under any type of loading.

Contents

1 Introduction

The two goal of this research are to prove that there is an initial interfacial stiffness dependency in the interfacial thick level set method and to make adjustments to this interfacial thick level set method regarding the constitutive relations within the interface elements. In this chapter the motivation of this research is given and the research objective is presented. Finally, an overview of the content of this report will be presented.

1.1. Background

Crack growth and subsequently delamination or rupture is an important failure mechanism in several materials. To simulate this failure mechanism, many numerical models have been developed in the framework of damage mechanics. Most models for delamination analysis are based upon the cohesive crack approach. This approach considers a small fracture process zone (FPZ) around the crack tip. Cohesive tractions are defined as a function of displacement jumps using a single simplified constitutive relation, the traction-separation law. Interface elements are used in finite element programs to implement the cohesive zone models. These elements define the discontinuity at the interface of a laminate or at the crack tip in metals for example [9]. Schellekens and De Borst [18] were the first to use interface elements in the context of delamination modeling.

There are currently two critical issues concerning the cohesive crack models. The first issue is the number of interface elements applied in the cohesive model. If the mesh is not sufficiently refined, the load-displacement response will not be smooth. Oscillations may appear in the response, leading to inaccurate results. However, small elements for analyses on structures of industrial scale will lead to excessive computational work. To overcome this problem Turon et al. [20] proposed to reduce the maximum interfacial strength, which results in a larger process zone. This enables an accurate simulation with an almost 10 times coarser mesh compared to an analysis with a nominal interface strength, while retaining an accurate simulation. However, a lower interfacial strength may lead to an overestimation of the predicted delamination area. For elastic-plastic material behaviour this can give issues as well. A lower interfacial strength means that the plastic strains are lower, which potentially can be an important factor for fatigue analysis with plasticity involved.

The second issue is related to extending cohesive zone models to fatigue analysis. Cohesive zone models are a successful technique for modeling monotonic fracture. However, the cohesive zone models are not capable of modeling the cyclic degradation observed in fatigue loading. In fact, the crack will automatically be apprehended in case of a constant amplitude load. This has given rise to a range of new cohesive zone models each with their own definition to ensure continuous crack growth under cyclic loading. Nguyen et al. [16], Roe and Siegmund [17] and Ural et al. [21] all came up with a new model. They all shared the common vision that damage evolution should somehow be related to fracture mechanics parameters and processes, albeit in different ways. However, the damage evolution laws are generally phenomenological in nature and damage and fracture are not clearly linked. An accurate extraction of the energy release rate is required to link the damage growth to Paris' law. The Paris law, which is fracture mechanics based, relates the stress intensity factor range to a crack growth rate. Therefore, damage mechanics and fracture mechanics should be linked to each other for fatigue analyses. Turon et al. [19] tried to bridge the gap between fracture and damage mechanics by relating the damage evolution to the empirical fatigue crack growth law. In his work, Paris'

law is evaluated at local level, through input of a local energy release rate. However, this is not a straightforward method since the conversion of local to global fracture parameters gives difficulties. Moreover, a local treatment can lead to localization and mesh dependency.

It is shown in several earlier works, like Voormeeren et al. [24] and Latifi et al. [8], that level set based models are a better match with the Paris' law and are also algorithmically more robust than continuum damage models, such as the cohesive zone model.

The most recent level set based model is the interfacial thick level set method (ITLS). This method has been proposed as a new approach for crack growth simulations and is suited to overcome the two issues regarding cohesive zone models. The ITLS requires the definition of damage as a function of distance to a damage front (see Fig. 1.1). There are several benefits to the ITLS model. One of the most valuable benefits is

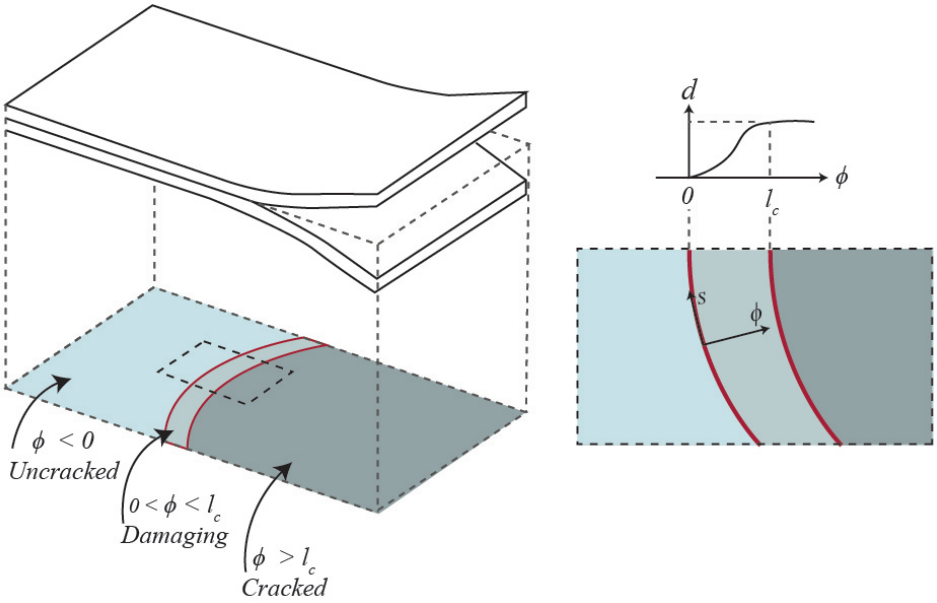

Figure 1.1: ITLS method: damage grows from 0 to 1 over a band with width l_c behind the level set front at $\phi = 0$ [8].

that it allows for robust evaluation of the energy release rate and straightforward implementation of a crack growth rate. For this reason the ITLS method is very suitable for fatigue crack growth analysis, since the Paris law describes the crack growth rate as a function of the energy release rate [8, 24].

The theoretical framework for the ITLS was developed by Latifi et al. [9] and uses a three dimensional (3D) formulation of the model. This can easily be reduced to a two dimensional (2D) formulation. For a 2D formulation the line describing the damage front, reduces to a single point, the crack tip. The damaged zone is a fixed length behind this point along which the undamaged material transforms gradually to a fully damaged material. The amount of damage at a certain location within the damaged zone is determined from the damage function, which is a function of the level set field ϕ. In this way crack formation is simulated. The interface elements are used to describe the crack path and have the advantage that the energy of the bulk is decoupled from the energy in the crack, which is related to the propagation of the crack.

1.2. Problem definition

The current ITLS model has proven to be a very robust and accurate model to simulate crack growth in quasi-static and fatigue load cases. However, the suspicion exists that there is a dependency on the initial interfacial stiffness for the global response of a system. The initial stiffness of the interface is a purely numerical parameter without a physical meaning and should therefore have no influence at all on the physical behaviour of the material.

The suspicion of a dependency on the initial interfacial stiffness is not discussed in any scientific works. However, in previous research by Voormeeren et al. [24], using an ITLS model with fatigue loading, different responses were observed when various values for the initial interfacial stiffness were adopted. The research showed that a variation of the initial interfacial stiffness influenced the predicted crack growth. This gives a

reason to suspect that the method is sensitive to the initial interfacial stiffness. Since this is the only research discussing the interfacial stiffness parameter explicitly, the sensitivity to this parameter should be investigated.

If a dependency on the initial interfacial stiffness for the current ITLS model can be proven, the next problem occurs. For the ITLS model to be an accurate and robust crack growth model, the dependency on the initial interfacial stiffness should be eliminated. This dependency would complicate the calibration procedure for identifying a suitable damage function for a given material, which is necessary for realistic crack formation. This motivates this research that will analyze the effects of the initial interfacial stiffness, with the aim to remove this spurious effect.

On top of the problem with the initial interfacial stiffness, the influence of plasticity on crack growth is of interest, since the suspicion for the initial interfacial stiffness dependency originates from fatigue analysis with plasticity involved. The general idea is that formation of a plastic zone around the crack tip influences the speed of crack growth. The residual plastic deformation can even lead to crack closure [5]. This happens for fatigue modeling with cyclic tensile loading. Plasticity also has an effect on the crack growth for quasi-static analysis. However, the effect is captured better through fatigue analysis with the use of an overload. Such an analysis can give more insight in the capability of the ITLS method to capture the influence of plasticity on crack growth in a specimen of a ductile material. When a solution can be found to the initial global stiffness issue, it would be interesting to investigate how an adapted ITLS model responds in a fatigue analysis. If the possible adjustments to the ITLS formulation are indeed applicable to fatigue analysis, the adapted ITLS model can be proposed as an accurate and robust approach for simulating crack growth under various loading types.

1.3. Research objective

The first research objective of this thesis is to investigate whether there is a sensitivity to the initial stiffness of the interface in the current ITLS model. If this is the case, the second objective becomes to remove the sensitivity to the initial interfacial stiffness. The choice for an initial interfacial stiffness should be decoupled from all other interfacial quantities, such as the damage function. To achieve the required results, the following research questions and sub-questions need to be answered:

1. Is there an initial interfacial stiffness dependency in the current formulation for the interfacial thick level set model?
    - I Are the effects significant for both linear elastic and elastic-plastic materials?
2. How can the formulation of the current ITLS model be adapted such that the effects on the global behaviour, resulting from the initial interfacial stiffness, are removed?
    - I Is it possible to adapt the formulation such that the renewed ITLS is applicable to both elastic and elastic-plastic materials in a quasi-static analysis?
    - II Does the adjusted method result in accurate solutions for different types of specimen and load cases?

1.4. Overview of report

This report is structured as follows: Chapter 2 presents the theoretical background of the cohesive zone and thick level set models. Chapter 3 presents a parameter study to investigate the dependency of the ITLS model on the initial interfacial stiffness. All parameters that are relevant to the behaviour of the interface are varied and compared. Chapter 4 presents an overview of two methods on improving the quasi-static ITLS model and results of a comparison between one of the formulated models and analytical solutions. Chapter 5 shows the results of the fatigue analyses with plasticity and an overload. Finally, in Chapter 6 conclusions and recommendations are presented.

2

Literature

In this chapter, the theoretical background that is needed to understand and improve the ITLS model is presented. In the first section the cohesive zone model with interface elements is discussed. Section 2.2 discusses the Thick Level Set (TLS) concept and subsequently the expansion to the ITLS model for two-dimensional (2D) analysis is explained in section 2.3. The ITLS model allows for several material models to be used. This research focuses on linear elastic and elastic-plastic material models. Linear elastic material models are very straightforward, plastic material models however need to be elaborated to broaden the understanding such that plasticity can be combined with fatigue for crack growth analyses. Therefore, the theory for fatigue analysis and plasticity in an ITLS model is needed, which is presented in sections 2.4 and 2.5. Finally, the type of loading used during the research is elaborated in section 2.6.

2.1. Cohesive zone method

The cohesive crack concept was first introduced by Dugdale [4] who considered a thin plastic plane in front of a notch. During the years the concept was elaborated to a finite element model by Hillerborg et al. [6]. The analysis of the initiation and growth of a crack under mode-I loading was carried out with this model. It was the basis for current cohesive zone models. In the current models it is assumed that a cohesive damage zone develops near the crack tip. The cohesive zone model (CZM) approach is characterized by the properties of the bulk material, the crack initiation condition and the crack evolution function. For the CZM a cohesive law is considered that relates the cohesive tractions to the displacement jumps along the crack plane. Damage initiation is related to the interfacial strength, τ^0, which is the maximum traction in the traction-displacement jump relation. The area beneath the traction-displacement jump relation is equal to the fracture toughness, G_c. There are several types of constitutive laws possible in cohesive elements, however the law with a bilinear relation between the tractions and displacement jumps is used most often (see Fig. 2.1). The initial slope of the constitutive relation is referred to as the initial interfacial stiffness, K [20].

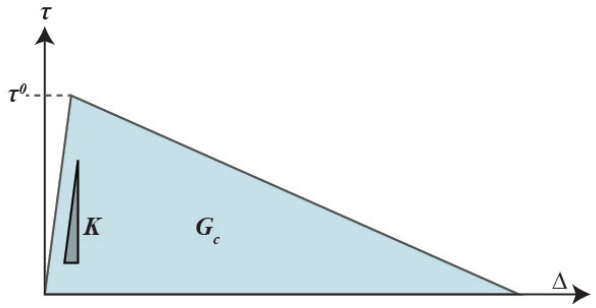

Figure 2.1: Bilinear cohesive law with initial stiffness K

In delamination models for 2D simulations crack growth is limited to a straight line and therefore cohesive damage models are mostly applied in combination with interface elements. In numerical models interface

elements are commonly used to describe a discontinuity along a predefined crack path. The damage is included in these interface elements by means of a damage parameter d, which describes the gradual decrease of the initial cohesive stiffness of the material. The cohesive stiffness then relates the displacement jump Δ to the corresponding cohesive traction τ, also known as the above mentioned constitutive relation for a cohesive zone model. The constitutive relation is derived from the definition of the free energy φ:

$$\varphi(\Delta, d) = \frac{1}{2}(1-d)\Delta^T K \Delta \tag{2.1}$$

$$\tau = \frac{\partial \varphi}{\partial \Delta} = (1-d)K\Delta \tag{2.2}$$

where K represents the initial cohesive stiffness. Since interface elements are used, the energy related to crack propagation is decoupled from the energy related to the bulk material, which makes the method also very convenient for problems involving plasticity.

The cohesive zone method has a limiting factor, which is the element size requirement. It is necessary to use a mesh with elements that are several times smaller than the cohesive zone length to assure robustness and accuracy. Clearly, such a requirement limits the size of the specimens that can be analyzed within an acceptable computation time [22].

2.2. Thick level set method

The thick level set (TLS) method is a method for modeling damage and fracture in solids. The TLS model was derived by Moës et al. [14] from the existing level set models as a continuum damage model. Similar to other continuum damage models a damage variable progressively reduces the stiffness of the material. However, in this method the damage variable is defined as a function of the distance to a moving front. This results in a moving band of damage. Furthermore, the model contains a non-local treatment to avoid spurious localization. Bernard et al. [2] improved the model to a robust and easy to implement model with an explicit damage growth algorithm. The main idea of the TLS approach is to locate a damaged zone in a material. This is where the advantage of the TLS lies: different damaged zones in a geometry can be captured through a single level set function. A level set function with multiple damaged zones is depicted in Fig. 2.2.

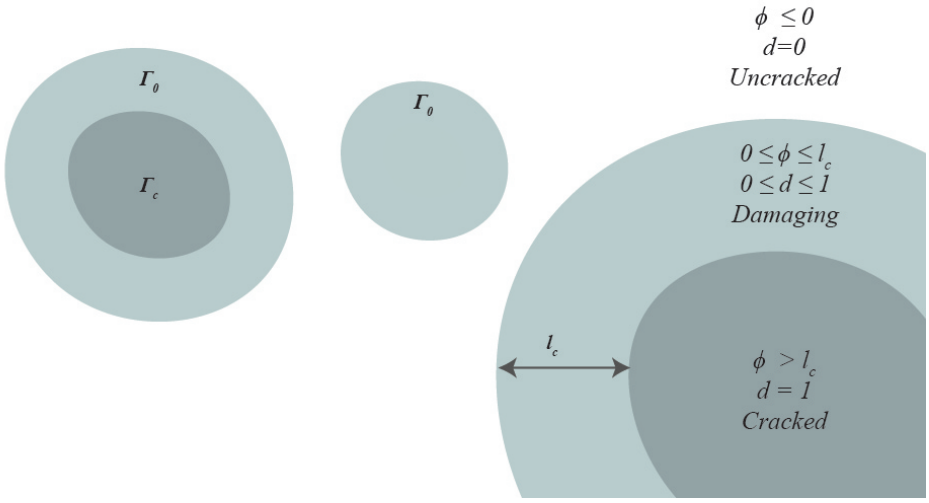

Figure 2.2: Example of multiple damaged zones with a single level set function in the domain Ω

The level set $\phi = 0$ separates the domain Ω into an undamaged and damaged zone. It is a signed distance function of which its value $\phi(x)$ is the minimum distance between x and the iso-zero of the level set field ϕ, called the damage front. In the damaged zone damage is considered a function of the level set field, $d = d(\phi)$. The damage runs from 0 to 1 as the level set field goes from 0 to l_c, respectively. This makes that the minimal distance between a point with $d = 0$ and a point with $d = 1$ is l_c, preventing aforementioned spurious

localization. Mathematically the damage is expressed as follows:

$$\begin{cases} d(\phi) = 0, & \phi \leq 0 \\ d(\phi) = 1, & \phi \geq l_c \\ d'(\phi) \geq 0, & 0 < \phi < l_c \end{cases} \tag{2.3}$$

Moës et al. [14] showed that the TLS approach is very promising for several reasons, of which a few are mentioned here:

- The non-local treatment is restricted to the damaged zones and it only requires a special treatment in the zone $0 \leq d \leq 1$, leading to lower computational costs.
- The transition from damage to crack is automatic, no additional computation is required.
- The TLS model is algorithmically robust due to the staggered solution scheme, which means that the displacements and damage are computed sequentially instead of iteratively.

Within the framework of the TLS, damage is automatically updated by describing a crack increment. The prescribed crack update implies an update of the level set ϕ, which successfully shifts the damage function.

Some characteristics of the quasi-static continuum TLS model are very suitable for 3D fatigue analysis, since the energy release rate can be computed non-locally and the crack growth rate is imposed from there. However, the continuum approach is not very suitable for 'normal' delamination analysis. Therefore, a discontinuous version of the TLS is developed for crack growth modeling under quasi-static (and fatigue) loading conditions. This new discontinuous version of the TLS is called the interfacial thick level set.

2.3. Interfacial thick level set method

The interfacial thick level set (ITLS) model can be seen as an adaption to the TLS model to provide an alternative to the cohesive zone model. Similar to the CZM, a traction-separation relation involving damage is assumed as the constitutive model of the interface. However, contrary to the CZM, damage is not an explicit function of the displacement jump across the surface but a function of a level set field ϕ on the interface. The level set field is defined in the same manner as for the TLS model as described in Eq. (2.3) [12].

The interfacial thick level set model is, as stated above, a discontinuous damage model for modeling crack growth along a predefined plane. Damage is applied to an initially stiff interface and the configurational force is computed from the displacement jumps of the interface. The use of interface elements accommodates the discontinuity of the model. Latifi et al. [9] found that the model results are not sensitive to the chosen width of the damaged zone, and if the width is increased the elements can be chosen larger. An independent stress based initiation criterion is introduced so that, in contrast with cohesive zone models, the size of the numerical FPZ can be increased to mitigate mesh requirements without causing spurious initiation of damage.

The solution algorithm for the ITLS model can be seen in Fig. 2.3. As mentioned before the TLS model provides a staggered solution scheme [2]. In the ITLS model this same staggered solution algorithm is adopted. The solution process starts with a given level set field $\phi(x)$. The iso-zero of the level set field implicitly defines the damage front location or, in the case of 2D, the crack tip location. Since for 2D situations the crack has reduced to a single line, the level set field is just the distance to the crack tip. The damage distribution follows from the given level set field through a predefined damage function $d(\phi)$. The displacement jumps (Δ) are obtained through standard finite element computation and the tractions (τ) are obtained through the constitutive relation for an interface element. This constitutive relation is described in Section 2.3.1.

Since the damage distribution is fixed, the displacement jumps can be used to compute the energy release rate (G) along the damage front. For 2D situations the damage front collapses into a point, the crack tip. This research focuses on 2D simulations, therefore the energy release rate is computed along a line, the damage band. This is done by numerical integration of the local energy release rate over the damaged zone. The computed energy release rate allows to compute the crack tip movement, which then is used to update the level set field. The new level set field values are then used in the next time step.

It has been shown that the ITLS model is very suitable for fatigue analysis. A crack growth rate can be imposed as the front velocity. This makes the method suitable for implementation of crack growth relations that relate crack growth rate to energy release rate, such as the widely used Paris' law for fatigue crack growth.

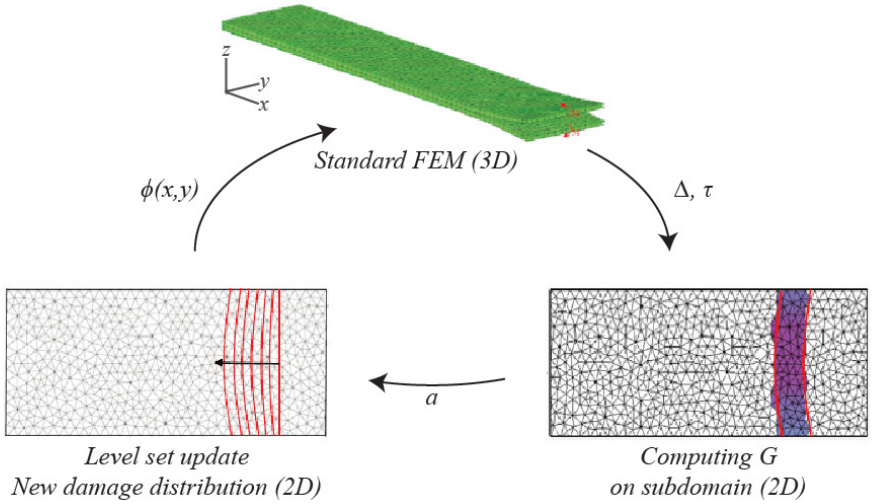

Figure 2.3: Solution algorithm for the ITLS model in 3D [9]

2.3.1. Local governing equations

For the CZM the definition of free energy was used to derive the constitutive law of an interface element (See Eq. (2.1)), which is copied in the ITLS model. The constitutive law of an interface element relates the displacement jump Δ to the traction τ in a material discontinuity. The free energy is expressed as:

$$\varphi(\Delta, d) = (1-d)\varphi_0\left(\Delta_i\right) - d\varphi_0\left(\delta_{1i}\langle-\Delta_1\rangle\right) \tag{2.4}$$

where $\Delta = (\Delta_1, \Delta_2)^T$ is a vector that contains the displacement jump in a local coordinate frame between the two facets of the interface. Δ_1 is the normal displacement jump and Δ_2 is the shear displacement jump. The scalar damage parameter d follows from the damage function, which is a function of the level set field (ϕ). This definition of the damage is different from the definition used in the cohesive zone method, where the damage is a function of the displacement jump. The variable φ_0 is defined as:

$$\varphi_0(\Delta) = \frac{1}{2}\Delta_i K \delta_{ij} \Delta_j \qquad i = 1,2; \qquad j = 1,2 \tag{2.5}$$

where K is the initial interfacial stiffness, which acts similar as the initial cohesive stiffness in a CZM model. The initial interfacial stiffness is a purely numerical parameter without a physical meaning that is present to ensure that the interface is stiff such that is does not contribute to the elastic deformation in a specimen before opening of the crack.

The traction at the discontinuity is obtained through differentiation of the free energy with respect to the displacement jump:

$$\tau_i = \frac{\partial \varphi}{\partial \Delta_i} = (1-d)K\delta_{ij}\Delta_j - dK\delta_{ij}\delta_{1j}\langle-\Delta_1\rangle \tag{2.6}$$

The local driving force is obtained by differentiating the free energy with respect to the damage:

$$Y = -\frac{\partial \varphi}{\partial d} = \varphi_0\left(\Delta_i\right) - \varphi_0\left(\delta_{1i}\langle-\Delta_1\rangle\right) \tag{2.7}$$

2.3.2. Damage definition

In Section 2.2 the damage definition of the TLS method is already briefly described. A length scale l_c is defined in the wake of the crack tip or front which determines the size of the damaged zone between the sane and fully damaged material (See Fig. 2.4).

The thick level set method provides the distance of every point inside the damage band to the crack tip using a signed distance function. The mathematical interpretation of the damage parameter was already given in Eq. (2.3). The damage $d(\phi)$ is a continuous function that can be differentiated on the domain ($0 < \phi < l_c$).

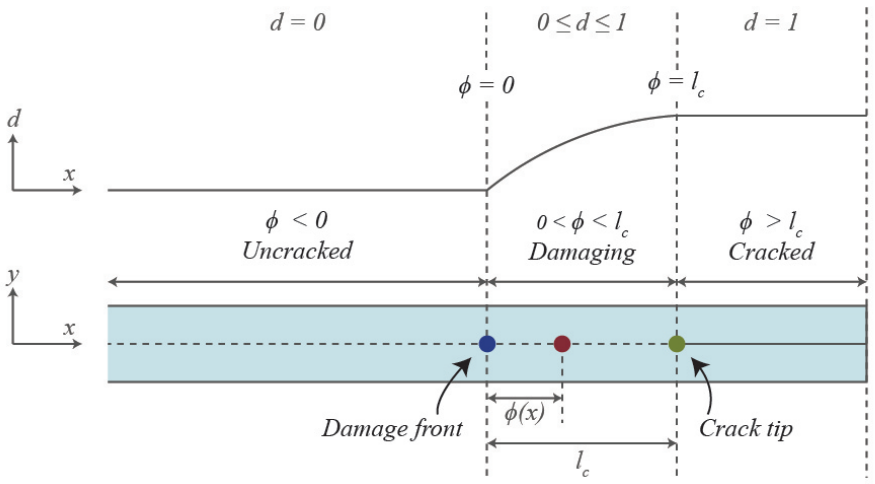

Figure 2.4: Damaged zone between sane and fully damaged material and damage distribution

There are several options for the definition of the damage function. In this research two definitions are adopted. The first damage definition was proposed by Bernard et al. [2]:

$$d(\phi) = \begin{cases} 0, & \phi \leq 0 \\ c_2 \arctan\left(c_1\left(\frac{\phi}{l_c} - c_3\right)\right) + c_4, & 0 < \phi < l_c \\ 1, & \phi \geq l_c \end{cases} \tag{2.8}$$

where satisfying the conditions given in Eq. (2.3) determines c_2 and c_4:

$$c_2 = \left(\arctan\left(c_1\left(1 - c_3\right)\right) - \arctan\left(-c_1 c_3\right)\right)^{-1} \tag{2.9}$$

$$c_4 = -c_2 \arctan\left(-c_1 c_3\right) \tag{2.10}$$

The parameters c_1 and c_3 are user defined, where c_1 determines the size and slope of the damage function

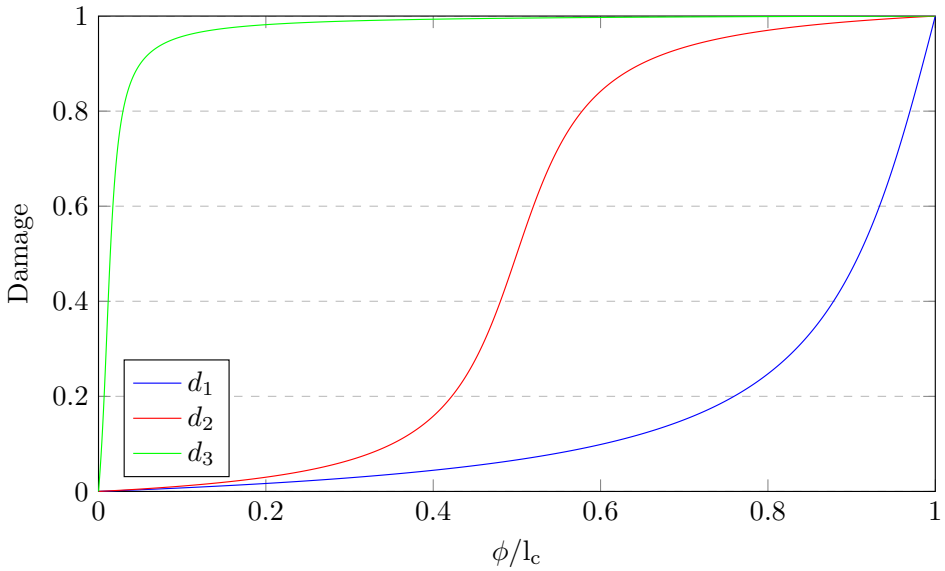

Figure 2.5: Three different shapes of the damage function as proposed by Bernard et al. [2]

and c_3 determines the location in the damaged band at which the damage starts to grow at a higher rate. The

damage function is governed by five parameters: l_c, c_1, c_2,c_3 and c_4. An example of three different shapes of this damage function is depicted in Fig. 2.5. The values for the user defined parameters c_1 and c_3 are ($c_1 = 10$, $c_3 = 1$) for d_1, ($c_1 = 15$, $c_3 = 0.5$) for d_2 and ($c_1 = 100$, $c_3 = 0.01$) for d_3.

The second damage definition was proposed by Voormeeren et al. [24]. It should be noted that this damage definition is equal to the first damage definition when the value for c_3 is set to zero.

$$d(\phi) = \begin{cases} 0, & \phi \leq 0 \\ \frac{1}{\arctan(c_1)} \arctan\left(c_1 \frac{\phi}{l_c}\right), & 0 < \phi < l_c \\ 1, & \phi \geq l_c \end{cases} \tag{2.11}$$

where the boundary conditions from Eq. (2.3) are met automatically. In this damage definition the user defined parameter c_1 determines the size and slope of the function. Opposite to the first damage function, this function is only governed by two parameters, l_c and c_1. The damage function is depicted in Fig. 2.6. The values for the user defined parameter c_1 are ($c_1 = 10$) for d_1, ($c_1 = 15$) for d_2 and ($c_1 = 100$) for d_3.

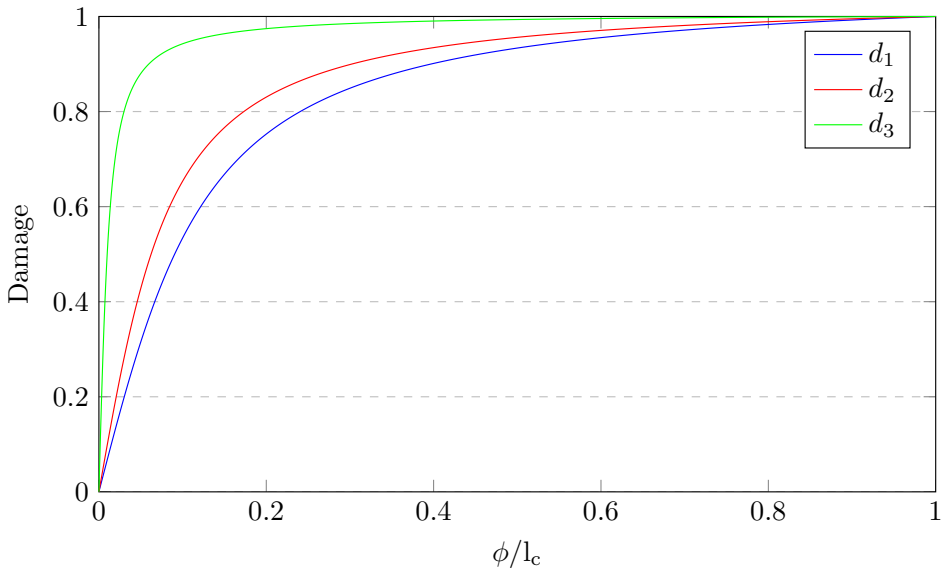

Figure 2.6: Three different shapes of the damage function as proposed by Voormeeren et al. [24]

2.3.3. Energy release rate

In the TLS approach the front energy release rate is computed by integrating the local driving force over the damaged zone. When the damage front moves infinitesimally from $A(0)$ to a new location A' in the sane material, the distance from any point $P(\phi)$ to the crack tip will change. Therefore, damage in these points, which is defined as function of shortest distance to the front, will be updated (See Fig.2.7). This results in a variation of the free energy in these points.

The energy G released due to the movement of A can be computed by integrating the local variation of free energy over the damaged band. For 2D, the integration takes place along a line:

$$G = -\int_0^{l_c} \frac{\partial \varphi}{\partial \phi} d\phi = -\int_0^{l_c} \frac{\partial \varphi}{\partial d} \frac{\partial d}{\partial \phi} d\phi \tag{2.12}$$

Using the definition of the local driving force in Eq.(2.7), the above equation can be rewritten to:

$$G = \int_0^{l_c} d'(\phi) Y d\phi \tag{2.13}$$

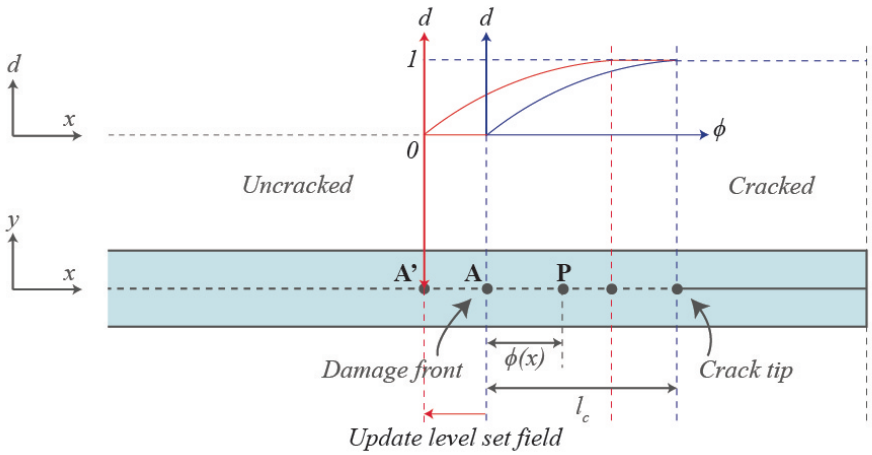

Figure 2.7: Updating damage distribution inside damage band due to an infinitesimal movement

where $d'(\phi)$ is the spatial derivative of the damage function. Eq.(2.13) enables us to compute the energy release rate at the damage front. Note that the integration domain only spans the region where the damage derivative is non-zero, i.e. the fracture process zone [24].

For the elementwise numerical integration of Eq.(2.13) a two-point Gauss integration scheme is used. However, during the movement of the damage band, the front ($\phi = 0$) and wake ($\phi = l_c$) can intersect the interface element. This causes an unsmooth damage distribution inside the element. In order to improve the accuracy and prevent unsmoothness, the interface element crossed by one of the boundaries of the damage band is sub-divided in two sub-elements. In both the sub-elements a two-point Gauss integration scheme is applied (See Fig. 2.8).

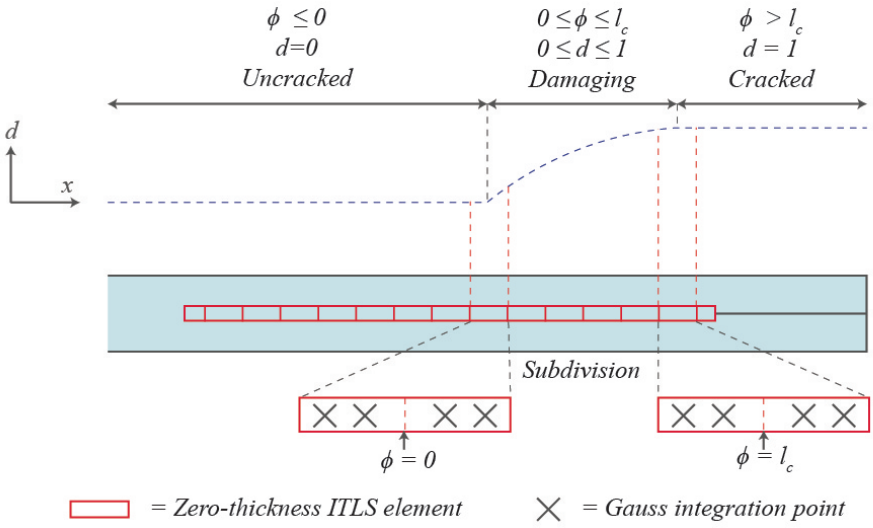

Figure 2.8: Sub-division of zero-thickness interface elements for ITLS model

2.3.4. Damage growth

In a level set method, the level set field needs to be updated after every time step. To update the damage distribution, the advance of the level set front should be related to the computed values for the energy release rate G and the resistance against crack growth G_c. The damage develops when the value for G is equal or even bigger than G_c at the tip. The change of the level set field is related to the normal velocity v_n of the front tip. In quasi-static simulations there is no actual time involved. Therefore, the ITLS does not directly work with velocities but with a front increment. In this case $v_n \Delta t$ is regarded as the front increment. To update the level

set field the following expression is used:

$$\phi^{n+1} = \phi^n + v_{\mathrm{n}} \Delta t \tag{2.14}$$

where the super-scripted n indicates the number of the time step and Δt is the time increment size. It should be noted that when the level set field ϕ^n in the previous time step n, which is a signed distance function, moves $v_{\mathrm{n}} \Delta t$ units forward in the normal direction, the updated level set field ϕ^{n+1} obtained from Eq. (2.14) is still a signed distance function.

In the TLS model defined by Moës et al. [14], Bernard et al. [2] and van der Meer and Sluys [22] the loading scheme was based on a unit load analysis in each time step. A critical load scale factor was computed using the assumption of secant unloading. However, this approach is not applicable when plasticity is involved. The framework of the TLS method had to be adapted for such cases. A relation for the normal velocity as found by Van der Meer et al. [23], Latifi et al. [9] and Mororó and van der Meer [15] was adopted:

$$v_{\mathrm{n}} = \frac{1}{\mu} \left\langle \frac{G}{G_c} - 1 \right\rangle_+ \tag{2.15}$$

where μ is a parameter that can be interpreted as a viscous resistance against crack growth. The Kuhn-Tucker conditions for quasi-static crack growth with $G - G_c \leq 0$ are approached in the limit of $\mu \to 0$. To denote the positivity condition the brackets are used, which reflects the irreversibility of crack growth. In order to ensure stability of the explicit level set update, Δt is reduced when this is necessary to limit the growth of the front with [23]:

$$\Delta t = \min \left\{ \Delta t^0, \alpha_{\mathrm{n}} \frac{h}{v_{\mathrm{n}}} \right\} \tag{2.16}$$

in which Δt^0 is the initial and maximum time step size and α_{n} is a constant with values $0 < \alpha_{\mathrm{n}} < 1$. α_{n} ensures that the crack growth per time step doesn't become bigger than the size of an element.

In case of a fully developed damaged band, movement of the front implies damage propagation. For this research a fully developed damaged band is used, which implies that there is only crack propagation and no crack initiation present in the model.

The fracture mode dependency of G_c, needed in Eq. (2.15), is taken into account by the expression introduced by Benzeggagh and Kenane [1]:

$$G_c = G_{\mathrm{I}c} + (G_{\mathrm{II}c} - G_{\mathrm{I}c})(\beta)^\eta \tag{2.17}$$

where η is a mode interaction parameter, G_{Ic} and G_{IIc} are the fracture energies in mode-I and mode-II. The mode ratio β is defined as:

$$\beta = \frac{G_{\mathrm{II}}}{G} = \frac{G_{\mathrm{shear}}}{G} \tag{2.18}$$

where G_{shear} is the value of the shear part of the energy release rate. The dependence of G on β and G_{shear} means that, apart from evaluating G, the shear part of the energy release rate also has to be computed to determine the damage update.

2.3.5. Solution scheme

The solution algorithm for the ITLS model with quasi-static loading is summarized in Fig. 2.9. There are a few items to be noted: (1) a damage band with length l_c is predefined ahead of the initial crack tip before the first displacement increment is applied; (2) a staggered solution scheme is used for the damage update and the displacement field, because of its robustness and simplicity. This means that the stresses and displacements are computed first, before updating the damage field. The solution scheme is sequential rather than iterative, introducing load step dependence in case of large step sizes.

1 Set the time step number $n = 1$;

2 Define an initial damage band with length l_c ahead of the crack tip and calculate the level set field $\phi(x)$;

3 Initialize the damage distribution on the level set field using Eqs. (2.8) or (2.11);

4 Set the initial time step Δt^0;

5 Apply the n^{th} displacement increment;

6 Compute displacement jumps Δ_i through standard FEM analysis and tractions τ_i through Eq. (2.6);

7 Compute the configurational force Y using Eq. (2.7) and subsequently G from Eq. (2.13);

8 Determine the crack velocity v_{n} from Eq. (2.15);

9 Set the time step size for the next time step t^{n+1} through Eq. (2.16);

10 Update the level set field in the crack growth direction with the use of Eq. (2.14);

11 Update the damage distribution with the updated level set field using Eqs. (2.8) or (2.11);

12 $n = n+1$, go to step 5 and repeat;

Figure 2.9: Solution algorithm

2.4. ITLS fatigue modeling

In case of quasi-static loading and fracture the crack will propagate when the energy release rate G exceeds the fracture energy G_c of the material. However, in case of fatigue the loads associated with crack growth are lower and crack growth is typically described by Paris' law [7]:

$$\frac{\mathrm{d}a}{\mathrm{d}N} = C\left(\frac{\Delta G}{G_c}\right)^m \tag{2.19}$$

where N is the number of cycles, ΔG the cyclic variation of energy release rate and C and m are material constants that can be determined from fatigue tests. The cyclic variation of energy release rate ΔG is defined as:

$$\Delta G = \left(1 - R^2\right) G \tag{2.20}$$

where G is obtained by solving Eq. (2.13) and R is the fatigue load ratio. Fig. 2.10 shows the logarithmic relation between the crack growth rate and normalized energy release rate. In fact, the Paris law is an empirical relation and not an actual law. It is however the most appropriate crack propagation criterion currently available and will be referred to as a law for this reason. The same constitutive framework and expression for

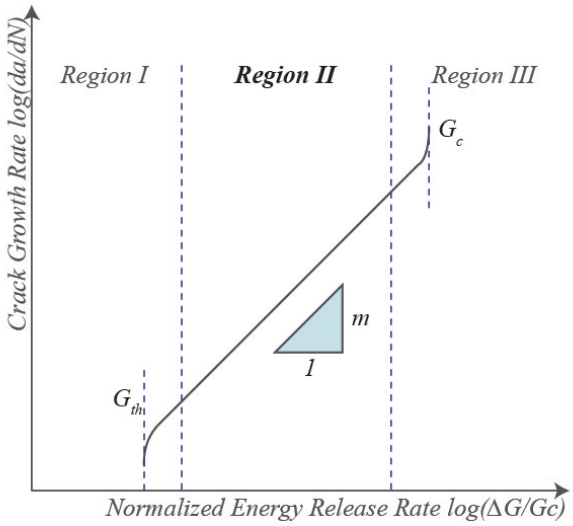

Figure 2.10: The Paris' law relates the crack growth rate to the normalized energy release rate in region II

the energy release rate as described in sections 2.3.1 and 2.3.3 are applicable to a fatigue crack growth analysis. The part that differs for the fatigue analysis is encapsulated in the damage growth model. It should be noted that modeling the full loading-unloading cycle is numerically impractical. Therefore, a loading envelope approach is used. This means that the maximum load is applied and the influence of the cyclic loading is incorporated through the Paris law, which is embedded in the model.

2.4.1. Damage growth model

As mentioned in Chapter 1, the ITLS (or TLS) model offers an elegant way to link damage to the fracture mechanics based crack growth model. Paris' law can be assessed for both linear elastic and elastic-plastic materials. The focus of this research will be on elastic-plastic materials. For elastic-plastic materials, slight adjustments have to be done to the Paris' equation and the loading scheme.

The nodal increase of the level set field follows from Eq. (2.14). The velocity however, is computed in a different manner for fatigue analysis. The change of the level set field is now related to the change of the cycles. This results in the following velocity:

$$v_{\mathrm{n}} = \left(\frac{\mathrm{d}a}{\mathrm{d}N}\right)\left(\frac{\mathrm{d}N}{\mathrm{d}t}\right) \tag{2.21}$$

where $\frac{\mathrm{d}a}{\mathrm{d}N}$ is the crack growth rate and $\frac{\mathrm{d}N}{\mathrm{d}t}$ is the time derivative of the cyclic function used.

The size of the time steps are computed with Eq. (2.16), which was also used for quasi-static analysis. The default value for Δt^0 is 1. When necessary the time step size is reduced to ensure that the crack growth per step does not exceed the limit, which is a fraction of the element length. The algorithmic aspects for the fatigue analysis are exactly the same as for the quasi-static analysis (See Fig. 2.9). The only difference between the two algorithms is the equation used in step 8, where Eq. (2.21) is used in this case.

2.5. Materials

Previously, interfacial crack growth behaviour studies have been done using the ITLS model on linear elastic (LE) material by Latifi et al. [9] and Voormeeren et al. [24]. The LE material used was a composite material, since this material is very sensitive to delamination of the plies. For this reason a composite material is used in all the LE simulations that were carried out during this research. Composite materials are orthotropic of nature, which means that the material properties differ in three mutually orthogonal directions.

The second focus in this research is on elastic-plastic (EP) materials, which has also been investigated by Voormeeren et al. [24] and Mororó and van der Meer [15]. For a perfectly sharp crack tip $\left(\lim l_c \to 0\right)$ the stresses are singular. In metals however, inelastic material behaviour will dominate the crack tip region by formation of a plastic zone. This will limit the stresses around the crack tip and will have an effect on the crack growth behaviour in the material.

Plastic behaviour is captured by means of a strain hardening model. In this study, it has been chosen to only consider isotropic hardening. Isotropic hardening increases the size of the yield function as shown in Fig. 2.11. For isotropic hardening the Lemaitre and Chaboche [11] model is adopted. This model increases

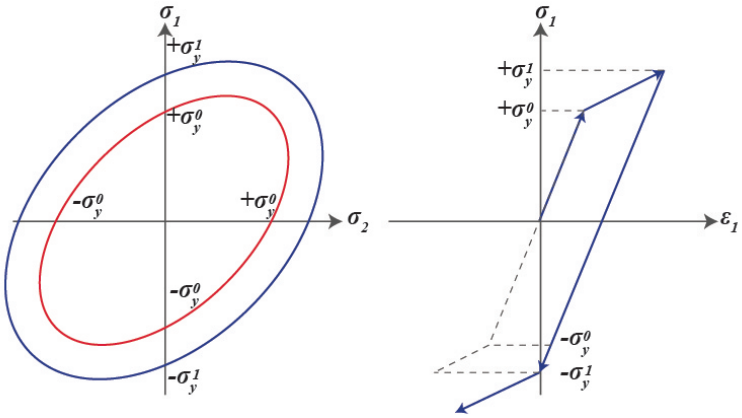

Figure 2.11: Isotropic hardening represented in the stress space, σ_y^0 is the initial yield stress and σ_y^t is the transformed yield stress

the yield surface as a function of the equivalent plastic strain:

$$\sigma_y^t = \sigma_y^0 + Q_\infty \left(1 - e^{-b_y p}\right) \tag{2.22}$$

where σ_y^0 is the initial yield stress, p represents the equivalent plastic strain, b_y is the rate of change of the yield surface and Q_∞ is the maximum change in size of the yield surface.

The effect of plasticity on the crack growth behaviour can be seen best through the use of an overload, which allows for the plasticity to grow while the crack remains at its position. The overload implies a fatigue analysis as described in 2.4.

2.6. Loading type

Within the field of fracture mechanics three different types of loading are distinguished; mode-I loading, mode-II loading and mode-III loading. For this research mode-III is not of interest, since 2D plain strain simulations are carried out and there is no loading in the third direction. However, a combination of mode-I and II can be made. The three possible modes are shown in Fig. 2.12. Mode-I is a loading normal to the crack plane, mode-II is the in-plane shear loading and the mixed mode combines the two load conditions. This research focuses on the mode-I loading, which implies tension dominated loading of the specimen.

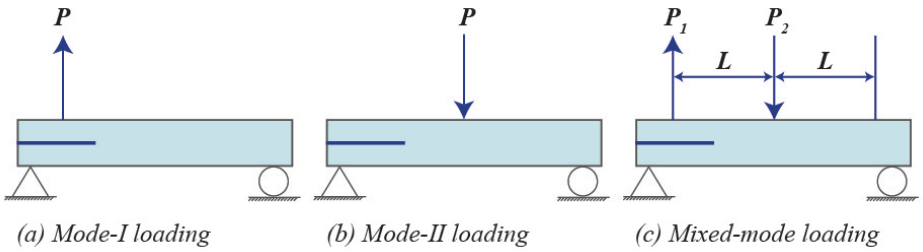

Figure 2.12: Loading conditions in three different fracture modes

3

Dependencies of the ITLS model

This chapter focuses on the the proof of the existence of a dependency of the ITLS method on the choice for the initial interfacial stiffness. A parameter study is carried out to obtain this proof for both linear elastic and elastic-plastic materials. All parameters that are relevant to the behaviour of the interface are discussed, after which conclusions are drawn about the influence of each individual parameter. This knowledge can then be used for adaption of the current ITLS model.

3.1. Input model

To be able to investigate the effect of each interfacial input parameter, a DCB test under plane strain conditions is modeled. The DCB test is common to determine the mode-I fracture toughness. Fig. 3.1 shows the boundary conditions of the simulations. The specimen was 102 mm long and 1 mm wide, which makes it equivalent to a two-dimensional (2D) simulation. The arms of the specimen are 1.56 mm thick and the initial crack is 32.9 mm long. In the vicinity of the crack large crack refinements are present. The elements have a size of 0.3 mm.

This geometry for the DCB test is used throughout the Chapters 3 and 4 for all simulations. Both a linear

Figure 3.1: 2D DCB specimen for simulating crack growth under quasi-static loading

elastic material and an elastic-plastic material were used in the simulations. The material properties for the LE material are related to a carbon/PEEK fiber reinforced composite and are listed in Table 3.1. The material properties for the EP material are related to the properties used by Voormeeren et al. [24] in his EP fatigue analysis. These properties are listed in Table 3.2.

Table 3.1: Material properties for carbon/PEEK fiber reinforced composite used in mode-I simulations

E_1	E_2	G_{12}	G_{23}	ν_{12}	G_{Ic}
122.7 GPa	10.1 GPa	5500 MPa	3700 MPa	0.25	0.969 N/mm

Table 3.2: Material properties for the elastic-plastic material used in mode-I simulations from Voormeeren et al. [24]

E	ν	Q_∞	σ_y^0	b_y	G_{Ic}
210 GPa	0.3	55 MPa	465 MPa	2.38	2.907 N/mm

3.2. Interface parameter study

In order to determine whether there is a dependency encapsulated in the current ITLS model on the choice for initial interfacial stiffness, the dependency of each parameter affecting the behaviour of the interface is investigated. Parameters affecting the interfacial behaviour originate from the chosen level set field ϕ. The influence of each parameter is investigated by varying only that parameter, while keeping all other input parameters and the mesh constant. Quasi-static DCB simulations are considered for all parameters.

3.2.1. Damage function

Three different damage functions following the damage definition as proposed by Bernard et al. [2] were considered, d_1, d_2 and d_3 (see Fig. 2.5). The damage definition as proposed by Voormeeren et al. [24] is not used, since it is equal to the first definition with a value of $c_3 = 0$ and has therefore no additional value in this parameter study. Only crack propagation is considered, since the length of the initial damage band l_0 can be dependent on the type of damage function that is used. Therefore, all simulations start with a fully developed damaged band with a length of $l_c = 3$ mm. The LE and the EP simulations have a different input dummy stiffness K, being $K = 10^6$ N/mm^3 for the LE material and $K = 10^7$ N/mm^3 for the EP material.

The damage profiles were obtained from Eqs. (2.8), (2.9) and (2.10). The damage function consists of four parameters, of which only parameters c_1 and c_3 are user defined input parameters. Parameters c_2 and c_4 ensure that the damage function satisfies the boundary conditions and are dependent on parameters c_1 and c_3. Therefore, only parameters c_1 and c_3 are of interest in this parameter study. Both parameters will be varied individually with the aim to obtain insight on the impact of these parameters on the global response of the DCB specimen. To be able to understand the impact each parameter has on the global response, it is necessary to show the influence each parameter has on the damage function and therefore on the damaged zone. The different damage functions for a varying parameter c_1 and c_3 are depicted in Fig. 3.2.

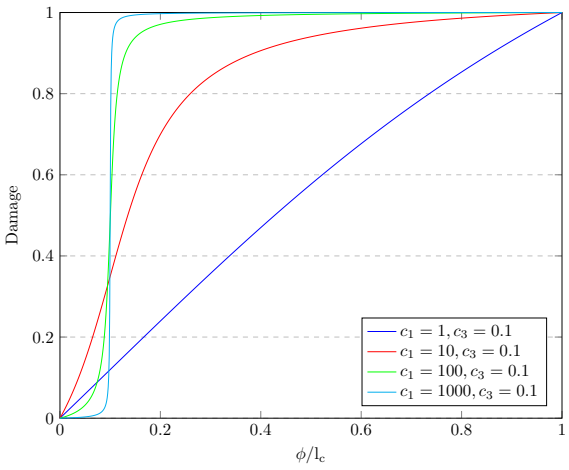

(a) Varying parameter c_1

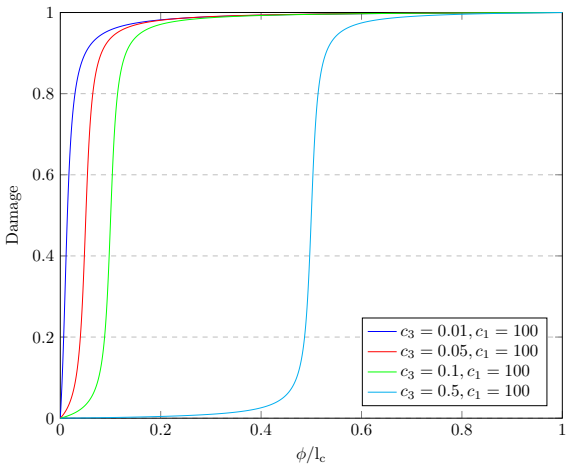

(b) Varying parameter c_3

Figure 3.2: Damage functions used for parameter study on the impact of varying damage parameters c_1 and c_3

In Chapter 2 it was already mentioned that parameter c_1 is responsible for the steepness of the damage function and therefore of the damage growth rate, which also becomes clear from Fig. 3.2a. Furthermore, it was mentioned that parameter c_3 is responsible for the location within the damaged zone at which the damage starts to grow at a higher rate. This is also the behaviour obtained from Fig. 3.2b. From both graphs it becomes clear that for a higher damage parameter c_1 the damage grows faster, whereas for a higher damage parameter c_3 the initiation of faster damage growth moves further away from the crack tip.

DAMAGE PARAMETER c_1

For this simulation, c_1 was varied, whereas c_3 remained constant. For all simulations c_3 had a value of 0.1. An increasing value for c_1 means that damage grows faster within the damaged band. The length of the damaged band and the initial interfacial stiffness are chosen to be equal to $l_c = 3$ mm and $K = 10^6$ N/mm^3 (LE) and $K = 10^7$ N/mm^3 (EP). Fig. 3.3 shows the load-displacement response for the DCB specimen with varying c_1 values for both the LE and EP material. A few issues can be remarked.

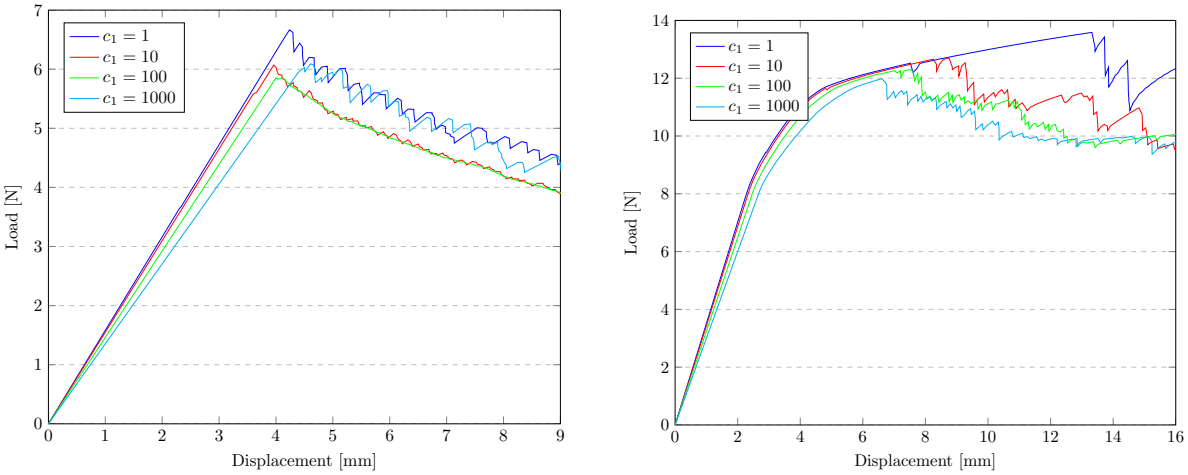

(a) Linear elastic material

(b) Elastic-plastic material

Figure 3.3: Comparison of load-displacement responses of the DCB specimen for different values of the damage parameter c_1

Firstly, the LE material response is discussed. The post-peak behaviour becomes smoother with an increasing c_1 with the only exception being $c_1 = 1000$. Furthermore, the $c_1 = 1$ and $c_1 = 1000$ variants give a slightly higher peak load and subsequently crack propagation branch. However, each c_1 value has the same average trend in the post-peak phase. The load-displacement response for $c_1 = 100$ gives the smoothest response in the post-peak phase. The smoothness of a response can be explained by examination of the integral in Eq. (2.13) that computes the energy release rate. The accuracy of this integral is related to the smoothness of its integrand $d'Y$ considering the given number of integration points inside the damaged band. Fig. 3.4a shows distribution of the product $d'Y$ over the length of the damaged band. The percentage of elements that the product $d'Y$ is distributed over is 20% for $c_1 = 1$, 45% for $c_1 = 10$, 82% for $c_1 = 100$ and 91% for $c_1 = 1000$. A smaller amount of elements means less integration points and less accuracy for computing the integral, which in turn explains a larger amount of oscillations. However, this does not explain the higher peak load and higher amount of oscillations of the simulation for $c_1 = 1000$. The cause for the higher peak load is the gradient of the damage profile. Due to the high value for c_1 the damage function is very steep and grows from a damage of 0 to 1 within the span of just 1 or 2 interface elements. This gives a maximum of 4 integration points to compute this gradient. Therefore, the solution becomes less accurate and sensitive to overshooting of the peak load. A solution to this problem could be to use smaller elements or to use higher order elements.

Secondly, the EP material is discussed. Again the post-peak behaviour of the load-displacement response becomes smoother with an increasing value for c_1. This time however, $c_1 = 1000$ is not an exception on this trend. Apart from the difference in the onset of crack propagation, $c_1 = 10$, $c_1 = 100$ and $c_1 = 1000$ seem to follow the same averaged trend. Due to the heavy fluctuations and the peak-load that is significantly higher than for the three other simulations, it is difficult to validate whether the averaged post-peak response trend for $c_1 = 1$ can be compared with the other three simulations. The higher peak load is caused by the relatively small growth of damage inside the damaged band. This results in a postponed crack initiation and therefore higher peak load. For the EP material the smoothness of the load-displacement responses can be explained as well by examination of the above mentioned integral. Fig. 3.4b shows distribution of the product $d'Y$ over the length of the damaged band. he percentage of elements that the product $d'Y$ is distributed over is 38% for $c_1 = 1$, 45% for $c_1 = 10$, 73% for $c_1 = 100$ and 92% for $c_1 = 1000$. Following the knowledge that a higher amount of contributing elements gives more accuracy for computing the integral and thus less oscillations, the results are as expected. The response for $c_1 = 1000$ delivers the smoothest response out of the four simulations. It should be noted that the chosen values for the initial interfacial stiffness differ between the LE and EP material. Therefore, the results should not be compared directly.

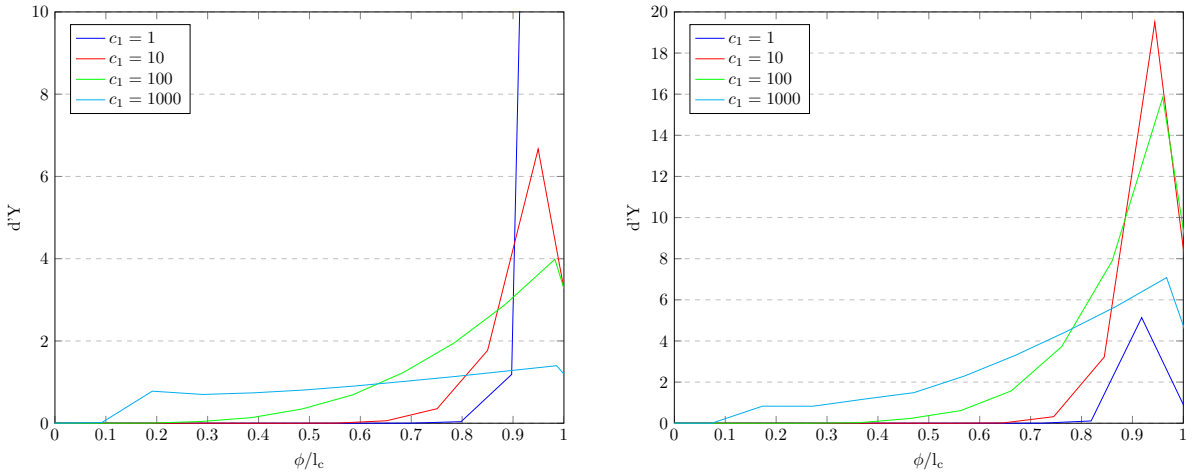

(a) Linear elastic material

(b) Elastic-plastic material

Figure 3.4: Variation of the product $d'Y$ along the length of the damaged band for different c_1 values

DAMAGE PARAMETER c_3

For this simulation, c_3 was varied, whereas c_1 remained constant. For all simulations c_1 had a value of 100 since this gave relatively smooth results in the simulations for a varying c_1 parameter. An increasing c_3 parameter results in the retardation of the damage growth. The value of c_3 determines where the damage begins to grow at a steeper rate. Fig. 3.5 shows the load-displacement response for the DCB specimen with varying c_3 values for both the LE and EP material.

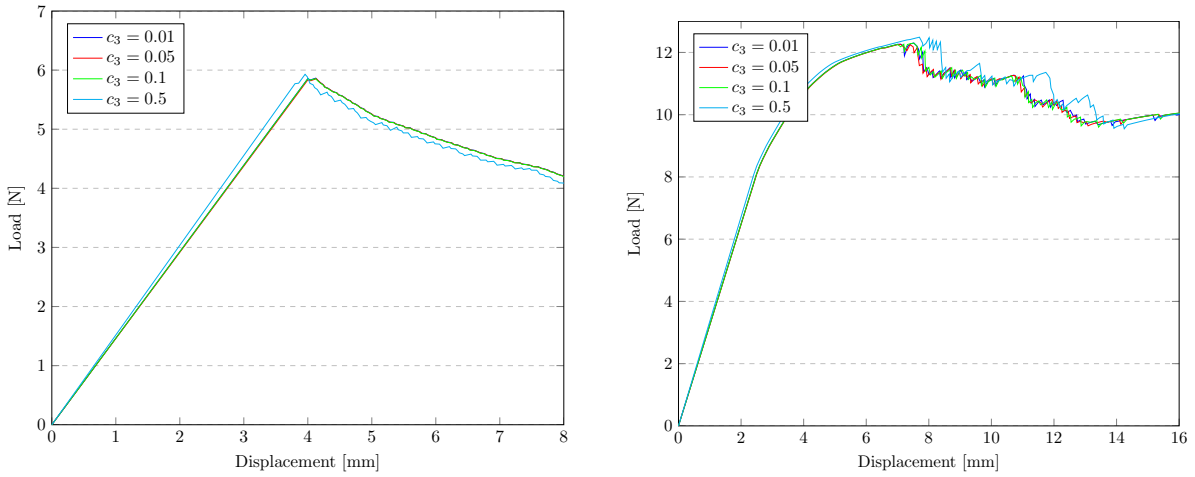

(a) Linear elastic material

(b) Elastic-plastic material

Figure 3.5: Comparison of load-displacement responses of the DCB specimen for different values of the damage parameter c_3

The results for the load-displacement response of the LE material show smooth results. Only for $c_3 = 0.5$ the post-peak response is less smooth compared to the other three values for c_3. Just as for the c_1 parameter, this can be explained by investigation of the energy release rate integral. The integrand $d'Y$ determines the smoothness of the load-displacement response. Fig. 3.5a shows the variation of the product $d'Y$ over the length of the damaged band. It becomes clear that for $c_3 = 0.01$, $c_3 = 0.05$ and $c_3 = 0.1$ the product $d'Y$ is distributed over approximately the same amount of elements. For $c_3 = 0.5$ this product is distributed over a lower amount of elements resulting in a less accurate computation of the energy release rate and therefore a less smooth post-peak load-displacement response. Looking at the trend of the responses, it can can be observed that for $c_3 = 0.01$, $c_3 = 0.05$ and $c_3 = 0.1$ the exact same response is obtained, where for $c_3 = 0.5$ the same averaged post-peak trend is obtained.

The simulations for the EP material show similar results to the LE results. Again the simulations are rel-

atively smooth with $c_3 = 0.5$ being the only response with slightly more oscillations and a slightly higher peak-load. The amount of oscillations is, as before, explained by the amount of elements contributing to the product $d'Y$. From Fig. 3.5b it can be seen that for $c_3 = 0.5$ the amount of elements is less than for the other c_3 parameter values. Hence a less smooth post-peak response is obtained. However, in general all four load-displacement responses have an equal averaged post-peak trend, where $c_3 = 0.01$, $c_3 = 0.05$ and $c_3 = 0.1$ even show the exact same response.

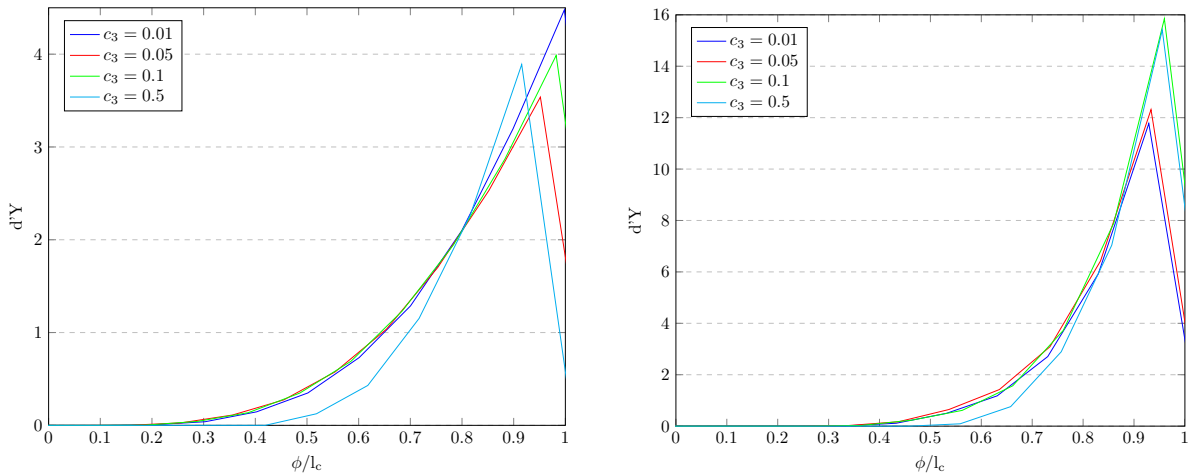

(a) Linear elastic material

(b) Elastic-plastic material

Figure 3.6: Variation of the product $d'Y$ along the length of the damaged band for different c_3 values

CONCLUSION
After reviewing all the obtained results for the simulations with a varying damage function a few conclusions can be made. The damage function as a whole has a significant influence on the load-displacement response for the DCB specimen for both the LE and the EP material. This influence relates to the global initial stiffness of the system, the value for the peak load and the amount of oscillations in the post-peak response. Since the damage function consists of two input parameters, both parameters where investigated individually to explore which parameter affects specific aspects of the global behaviour. The results indicate that c_3 has almost no influence on the global response. The influence only becomes evident when the value for c_3 is 0.5 or higher. In further simulations no values of $c_3 \geq 0.5$ will be used due to the fact that it gives less smoothness of the response and it gives a damage profile less similar to damage in cohesive methods then for lower c_3 parameter values. It can be concluded that for c_3 values lower than 0.5 the load-displacement response is not influenced by this damage parameter.

The input parameter c_1 has a significant influence on the results. The first conclusion is that an increasing value for c_1 results in a decreasing global initial stiffness. The second conclusion is that an increasing value for c_1 results in less oscillations in the post-peak response of the specimen. However, care must be taken when increasing the value for c_1. There seems to be a certain threshold and exceeding this threshold results in higher peak loads and more oscillations. The load-displacement response for $c_1 = 1000$ in Fig. 3.3a shows this behaviour.

3.2.2. Length of the damaged zone

From a numerical point of view the length of the damaged band l_c determines the number of elements inside the band for a given constant mesh. To investigate the sensitivity to the amount of elements inside the damaged band on the results, 2D simulations of the DCB test were conducted with four different values for l_c. The initial interfacial stiffness was set as K = 1e6 N/mm^3 for the LE material and K = 1e7 N/mm^3 for the EP material. Fig. 3.7 shows the load-displacement responses for a varying length of the damaged zone for two different materials. For both materials the results are similar. It is observed that with the increase of l_c from 2 mm to 5 mm the oscillatory response converges to a slightly smoother response due to the fact that the computation achieves a higher accuracy when the number of elements in the damaged zone is increased. The element size for all computations was 0.3 mm, yielding approximately 7, 10, 14 and 17 elements along the length of l_c.

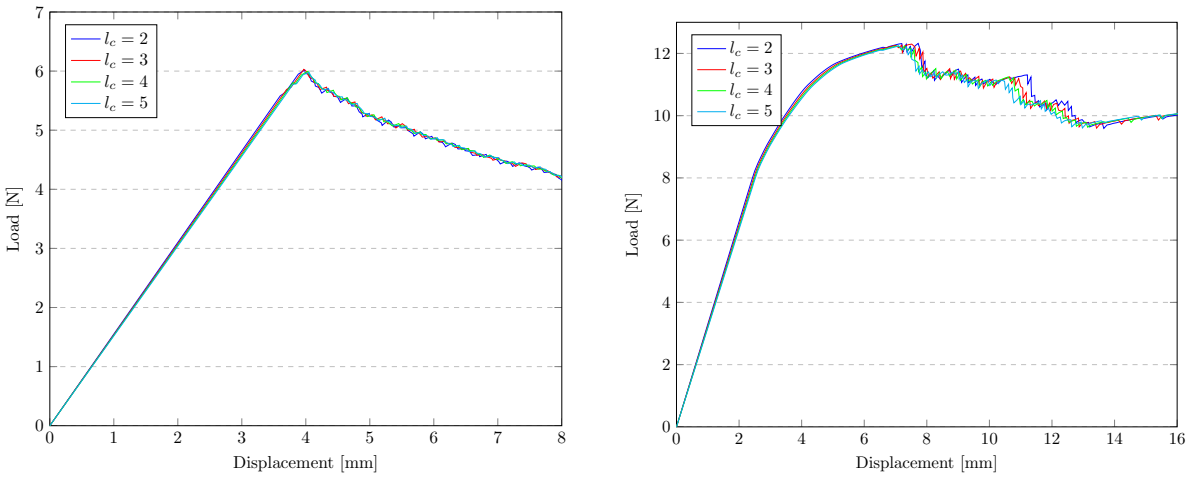

(a) Linear elastic material

(b) Elastic-plastic material

Figure 3.7: Comparison of load-displacement responses of the DCB specimen for different lengths of the the damaged band l_c

It should be noted that the results from Fig. 3.7b are somewhat surprising. For smaller values of l_c the stresses around the crack tip should be higher, which would then result in more plasticity. From the curves it can be seen that this also applies to the performed simulations. However, the observed effect is small. The reason for the relative small effect could be caused by the choice for the damaged zone parameters. When l_c becomes larger the load that has to be carried by the damaged zone is distributed over a larger surface, which would be visible in the load-displacement curves by a smaller hardening part. In this particular situation the choice for the damaged zone parameters could be such that for a decreasing l_c the part of the damaged zone responsible for transferring the load does not decrease much in length. It is possible that the effect is visualized better when a smaller l_c than the values used for this research is chosen. Research on the traction distribution over the damaged zone for varying lengths of the damaged zone is a possible way of investigating if the length over which the forces are distributed inside the damaged band is only changing slightly for varying lengths of the damaged zone for a chosen parameter set. Along with such a research also smaller values for l_c could be used to investigate whether the plasticity effect becomes clearer for smaller lengths of the damaged zone.

CONCLUSION
Two conclusions are drawn from the comparison between different values for the length of the damaged zone l_c. Firstly, it can be concluded that the freedom to choose l_c is an advantage of the ITLS model that provides the possibility to use a coarser mesh resulting in lower computational costs while maintaining an equal accuracy and smoothness of results. This accuracy and smoothness can even be higher due to a higher amount of elements and therefore integration points within the damaged band.

Secondly, the length of the damaged band has no influence on the response of the DCB specimen. All simulations show curves that can be assumed equal. The minor differences that are present are only observed for the EP material and are negligible for this particular study. As mentioned, further research is needed on the surprising behaviour obtained for the EP material.

3.2.3. Initial interfacial stiffness

The initial interfacial stiffness K has no physical meaning. It is a purely numerical parameter to ensure that there is initially contact between the adjacent arms of the specimen. Furthermore, the parameter K provides that no deformations occur at the interface in the elastic region of the response. The deformations can only occur when the crack actually begins to grow.

Fig. 3.8 shows the load-displacement response of the DCB specimen with four different values for the initial interfacial stiffness K and for two different materials. The LE and the EP material display similar behaviour for the initial stiffness of the DCB specimen, the peak-load and the amount of oscillations. The initial global stiffness of the DCB specimen becomes higher with an increasing initial interfacial stiffness K. The oscillations and peak load increase as well with a growing stiffness K, where K = 1e9 N/mm^3 has a significantly higher peak load for both materials. However, the post-peak averaged trend is relatively the same for

all values of K. This is more evident for the LE material but also the EP material seems to acquire a similar post-peak trend for all four values of K. Since the post-peak response for the EP material is significantly more irregular than for the LE material it is difficult to judge whether there is indeed an equal averaged trend.

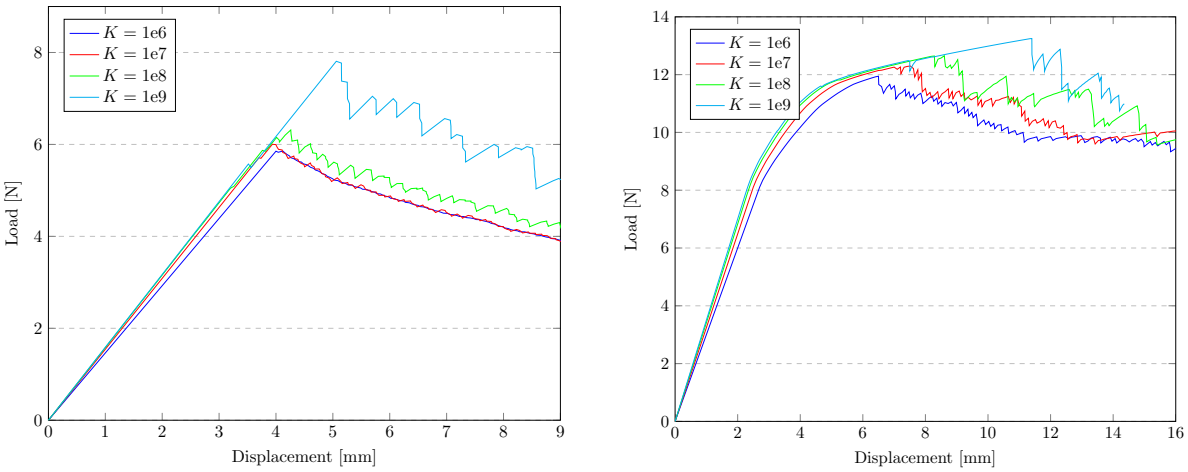

(a) Linear elastic material

(b) Elastic-plastic material

Figure 3.8: Comparison of load-displacement responses of the DCB specimen for different initial interfacial stiffnesses K

The increasing amount of oscillations are as expected when the variation of the product $d'Y$ is plotted. Fig. 3.9a shows the product $d'Y$ for the LE material and Fig. 3.9b shows the same product for the EP material. With an increasing value for K the amount of elements that contribute to the computation of the integral for the energy release rate decreases. The accuracy of the computation becomes less and more oscillations are observed. The peak-loads increase as well, the cause for this is the value for damage parameter c_1. If c_1 becomes too small compared to the initial stiffness K the damage growth is not steep enough anymore, resulting in a stiffer interface and a crack initiation at a later stage. This also means a higher peak-load. There seems to be a certain relation between parameters c_1 and K, which results in certain threshold values for both parameters. This is not a real threshold, it is more like a transition, since both parameters affect and reinforce each others behaviour.

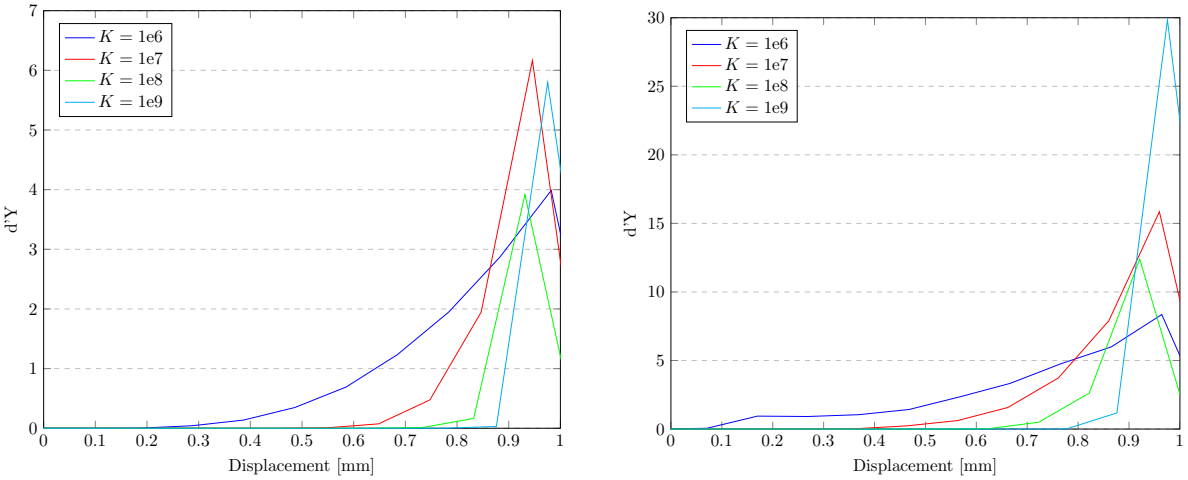

(a) Linear elastic material

(b) Elastic-plastic material

Figure 3.9: Variation of the product $d'Y$ along the length of the damaged band for different c_3 values

CONCLUSION

From the simulations for a varying initial interfacial stiffness K a few conclusions are made. The choice for the value of parameter K has a significant impact on the global response of the specimen. An increase of

the interfacial stiffness implies an increase in the global stiffness of the specimen. Whereas the peak load increases as well. The increase of the peak load is not of an significant order in most cases but for the initial interfacial stiffness of 10^9 N/mm^3 the increase is significantly higher compared to the other three stiffnesses. However, this could be explained by the influence the damage parameter c_1 has on the initial interfacial stiffness. The value for the c_1 parameter can not become too low compared to the input value for parameter K. There is a certain threshold when it comes to the possible combinations of values for the parameters c_1 and K. An elaborate parameter calibration should prevent inaccurate results.

3.3. Conclusion

After comparing all parameters related to the interface of the DCB specimen a few conclusions can be drawn. The first one is that the length of the damaged zone has no influence on the response of the DCB specimen. It should be noted that the chosen length should be in reasonable bounds relative to the length of the chosen specimen. No simulations with an extremely low or high length of the damaged zone were conducted. It lies within reason that this would have an influence on the global response of the DCB specimen.

The second conclusion is that both the chosen damage function as the initial interfacial stiffness has a significant influence on the global response. The influence of the damage function can be split into two input parameters. Where the c_1 parameter has a significant impact on the global behaviour and the c_3 parameter has a negligible impact on this behaviour. The c_1 parameter individually has an impact on the initial stiffness of the load-displacement response of the DCB specimen. With an increasing c_1 parameter the initial stiffness of the system reduces. The initial interfacial stiffness parameter K results in an opposite trend regarding global behaviour, an increasing K results in a higher initial stiffness of the system.

The last conclusion is that both the damage parameter c_1 and the initial stiffness parameter K have a joint influence on the global behaviour. This influence is not only related to the initial stiffness of the system but also yo the accuracy of the response. When the combination of values for c_1 and K is not chosen correctly the peak load will go up and the amount of oscillations in the post-peak response becomes higher.

4

Adapting the ITLS model

This Chapter presents two new ITLS models for the removal of the dependency of the numerical results on the initial interfacial stiffness K in the current model. The first model is formulated based on a different constitutive relation for the interface. The second model is formulated based on the assumption that there is a behavioural connection between the damage parameter c_1 and the initial stiffness parameter K. Both methods are validated and discussed after which one of the two models is chosen as the solution to the current problem of the ITLS model. The traction computed by the ITLS model will also be discussed briefly. A comparison with a CZM model is carried out to evaluate the obtained traction qualitatively. Finally, the adapted ITLS model is compared to an analytical solution to validate the accuracy of the improved model.

4.1. Introduction to solution methods

In the previous Chapter it was proven that the choice for the initial interfacial stiffness is dependent on the choice for the damage function for the current ITLS model. When a certain damage function is chosen, a varying initial interfacial stiffness results in a different initial stiffness of the specimen. Since for all simulations that were conducted the bulk material remained the same, the dependency on the initial interfacial stiffness is assumed to be encapsulated in the response of the interface elements. The constitutive relation of the interface should be examined to investigate where the dependency on the initial interfacial stiffness and the damage function occurs. The constitutive law for interface elements was described in Section 2.3.1. For this reason an adaption of the constitutive law is presumed to be one of the possibilities to remove the dependency on the initial interfacial stiffness. Section 4.2 describes the investigation of the constitutive relations. This investigation to a new ITLS model will be referred to as method 1.

Secondly, one other method is used to remove the initial interfacial stiffness dependency. From previous Chapter it became clear that both the damage parameter c_1 and the dummy stiffness K have an influence on the global response of the DCB specimen. The possibility that these two parameters influence each other and therefore the global response is investigated. This could lead to a different definition of the damage function in the ITLS model. The derivation of the method is described in Section 4.3. This method will be referred to as method 2.

For all simulations executed in this Chapter a few parameters relating to the interface remained constant. The length of the damaged zone l_c and the damage parameter c_3 proved to be of no influence on the global response for the DCB specimen. Therefore, constant values for these two parameters were adopted, $l_c = 3$ mm and $c_3 = 0.1$. The material parameters are as described in Tables 3.1 and 3.2.

4.2. Adapted interfacial stiffness formulation - Method 1

It is assumed that an adaption of the constitutive relations can result in the removal of the initial interfacial stiffness dependency. To be able to adapt the model, a good understanding of the constitutive law of the interface is necessary. Therefore, the definition of the constitutive relations for method 1 are rewritten with a new expression for the interfacial stiffness.

4.2.1. Adapting the constitutive relations

All constitutive relations for an interface element are derived from the definition of free energy in Eq. (2.4). In literature all definitions for the free energy break down to relating a damage parameter, determined by a certain damage function, to an initial stiffness parameter. Since the goal is to remove the dependency on the initial stiffness and there is no other definition of free energy without containing an initial stiffness, a new definition for free energy is proposed. Replacing the stiffness parameter K by $\frac{K}{d}$ is explored as an option. Where d is the damage parameter and K is the same stiffness parameter as in the initial definition. The expression for the free energy becomes:

$$\varphi(\Delta, d) = \frac{1-d}{d}\varphi_0\left(\Delta\right) - \left(\frac{1-d}{d} - \frac{1-d_0}{d_0}\right)\varphi_0\left(\delta_{1i}\langle-\Delta_1\rangle\right) \tag{4.1}$$

which had to be adjusted compared to the expression as introduced in Section 2.3.1. To ensure that significant interfacial interpenetration due to negative displacement jumps in the normal direction is prevented, the d in the second term on the right-hand side needed to be replaced by $\left(\frac{1-d}{d} - \frac{1-d_0}{d_0}\right)$, where the d_0 is the lower bound of the damage. This lower bound is described in more detail in Section 4.2.2. The expression for the variable φ_0 could remain the same, which is defined as:

$$\varphi_0(\Delta) = \frac{1}{2}\Delta_i K \delta_{ij} \Delta_j \qquad i = 1,2; \qquad j = 1,2 \tag{4.2}$$

Due to the adapted expression for φ the traction and the local driving force change. The new expressions for both become:

$$\tau_i = \frac{\partial \varphi}{\partial \Delta_i} = \frac{(1-d)K}{d}\delta_{ij}\Delta_j - \left(\frac{1-d}{d} - \frac{1-d_0}{d_0}\right) K \delta_{ij}\delta_{1j}\langle-\Delta_1\rangle \tag{4.3}$$

$$Y = -\frac{\partial \varphi}{\partial d} = \left(1 + \frac{1-d}{d}\right)\frac{\varphi_0(\Delta_i)}{d} - \left(1 + \frac{1-d}{d}\right)\frac{\varphi_0\left(\delta_{1i}\langle-\Delta_1\rangle\right)}{d} \tag{4.4}$$

The new expressions of φ, τ and Y are less elegant as in the previous constitutive relations. However, these expressions ensure that there is no unphysical interpenetration in the model, while the new stiffness $\frac{K}{d}$ can be implemented.

4.2.2. Damage definition

Since the damage parameter d appears in the denominator in the expressions for the traction τ and the local driving force Y, the definition for the damage should be adopted. It not longer possible to have a damage growing from 0 to 1. Therefore, the bounds for the damage should be adapted, which leads to a slightly different determination of the c_2 and c_4 parameters in the damage function from Bernard et al. [2]. The new expression for the damage should satisfy the following:

$$\begin{cases} d(\phi) = l_{\text{bound}}, & \phi \leq 0 \\ d(\phi) = 1, & \phi \geq l_c \\ d'(\phi) \geq 0, & 0 < \phi < l_c \end{cases} \tag{4.5}$$

where l_{bound} is a parameter that determines the lower bound of the damage, which can be varied. Therefore, in this definition the damage in the sane material is equal to l_{bound} and increases to 1 in the fully damaged material.

Due to the change of the boundary conditions for the damage function, the parameters c_2 and c_4 are adapted such that they are satisfying the new boundary conditions:

$$c_2 = \left(1 - l_{\text{bound}}\right)\left(\arctan\left(c_1\left(1 - c_3\right)\right) - \arctan\left(-c_1 c_3\right)\right)^{-1} \tag{4.6}$$

$$c_4 = l_{\text{bound}} - c_2 \arctan\left(-c_1 c_3\right) \tag{4.7}$$

The new definition for damage is implemented in the numerical code for the ITLS, which makes the method suitable to run simulations with.

4.2.3. Comparison with current ITLS

The first thing that needs to be checked for this new method is the similarity with results from the current ITLS model. The method needs to be able to generate the same crack propagation path when the same parameters are used for both methods. For damage parameter c_1 a value of 100 is chosen, while parameters c_3 and l_c are chosen as described in Section 4.1. Fig. 4.1 shows the load-displacement responses for the current ITLS and for the new method with $\frac{K}{d}$. Both the LE and the EP material can be seen. From the two graphs it becomes clear that the load-displacement responses are similar for the two methods.

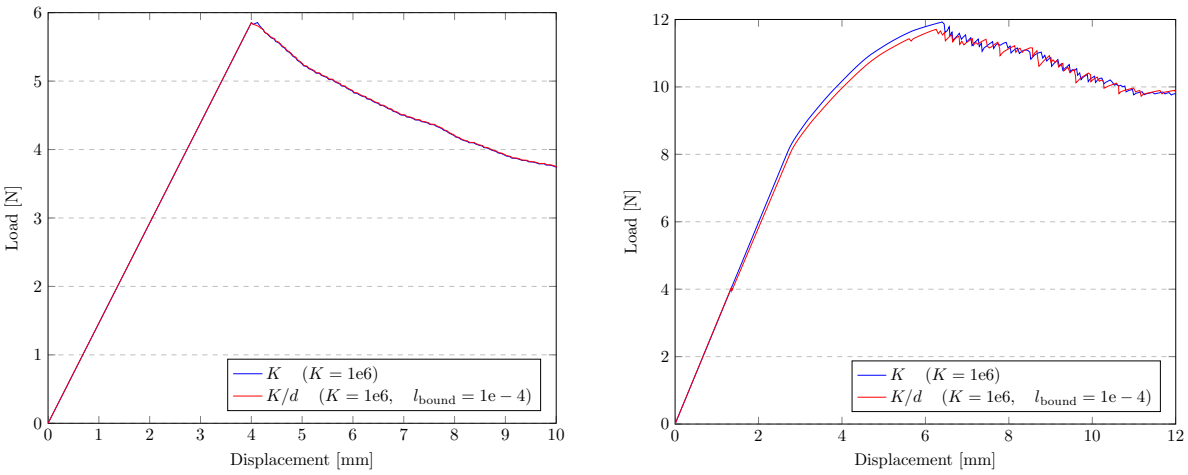

(a) Linear elastic material

(b) Elastic-plastic material

Figure 4.1: Comparison of load-displacement responses of the DCB specimen for a stiffness K and K/d

Due to the new formulation for damage it is possible to achieve a higher initial interfacial stiffness in the fully sane material, while obtaining the exact same global response for the the DCB specimen. For the new formulation the initial interfacial stiffness is determined as:

$$K_{\text{init}} = \frac{(1-d)K}{d} \tag{4.8}$$

This formulation and the fact that the lower bound for the damage is not zero but very small, $l_{\text{bound}} = 1e-4$ in the responses in Fig. 4.1, gives an initial stiffness in the sane material that is higher compared to the current ITLS model. The new method has an initial interfacial stiffness of $K_{\text{init}} = 9.999e9$ N/mm^3, whereas the current method has a stiffness of $K_{\text{init}} = 1e6$ N/mm^3. After the parameter study done on a varying initial interfacial stiffness (see Section 3.2.3), one would expect that such a large difference in stiffness would also show a difference in the global response of the specimen. The absence of dissimilarities in the responses for both methods can be explained by the initial stiffness over the length of the damaged band. In the case of the executed simulations a damage function was used that had a very steep growth of damage near the crack tip. Therefore, the damage is very close to 1 over a major part of the damaged band. From Eq. (4.8) it is observed that the damage parameter is in the denominator and dividing by a value close to or even equal to 1 reduces the interfacial stiffness over the damaged zone to a similar interfacial stiffness as for the current ITLS model. Section 4.2.4 will visualize this behaviour.

It should be noted that when using a damage function that does not have a steep growth to a damage of 1, the response could also have less similarity with the response for the current ITLS model when the same value for the dummy stiffness K is used.

4.2.4. Validating adapted interfacial stiffness

Since method 1 has proven to be a method that produces a similar global response compared to the current ITLS model, the method should now be validated as a possible solution to the problem of the initial interfacial stiffness dependency. This is done by executing simulations with varying values for the parameters K and l_{bound}. If this method is a solid solution to the problem, the responses should be exactly the same independent of the chosen values for K and l_{bound}.

The first parameter that is discussed is the stiffness parameter K. Fig. 4.2 shows the load-displacement responses for a LE and EP material with a varying value for the stiffness parameter K. It becomes evident that

partly the the same behaviour is obtained as from the simulations with a varying K in Section 3.2.3. The initial stiffness of the global response increases with the increase of the interfacial stiffness parameter K. However, regarding the peak loads for the different values of K an opposite behaviour is obtained. Whereas the current ITLS model resulted in higher peak loads for higher initial interfacial stiffness values, the new model results in higher peak loads for lower initial interfacial stiffness values. Generally a higher value for the initial stiffness K leads to higher stress concentrations around the crack tip. Therefore, crack initiation is reached earlier and a lower peak load is achieved.

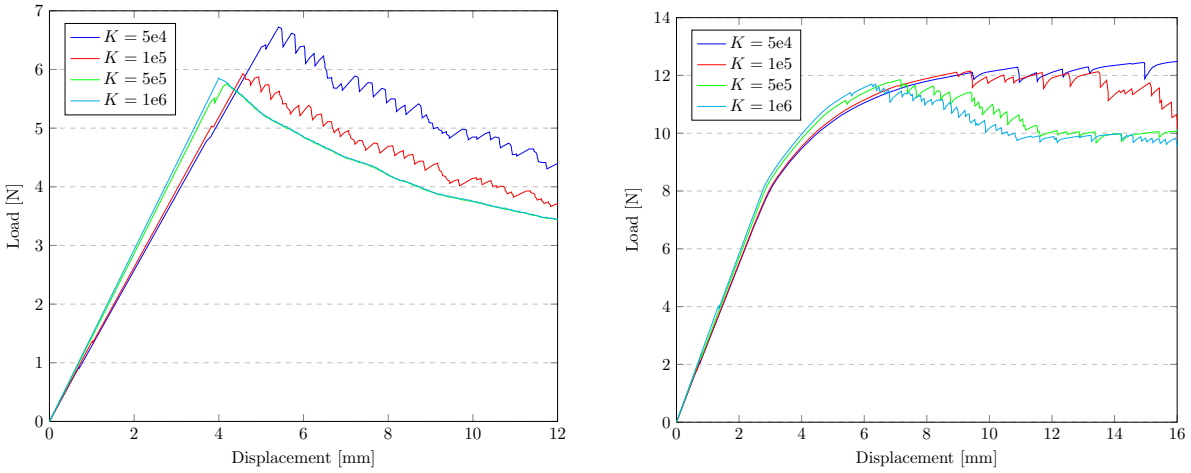

(a) Linear elastic material

(b) Elastic-plastic material

Figure 4.2: Comparison of load-displacement responses of the DCB specimen for a varying stiffness parameter K

The variation of the lower bound of the damage l_{bound} is discussed next. Fig. 4.3 gives the load-displacement response for the LE and EP material. The graphs show a perfect resemblance between the simulations with different values for the lower bound of the damage. It can be concluded that the new definition for the bounds of the damage, specifically the value for l_{bound}, has no influence on the global response of the DCB specimen. This supports the statement that the addition of the damage parameter d in the denominator of Eq. (4.8) has a negligible influence on the development of the interfacial stiffness inside the damaged band.

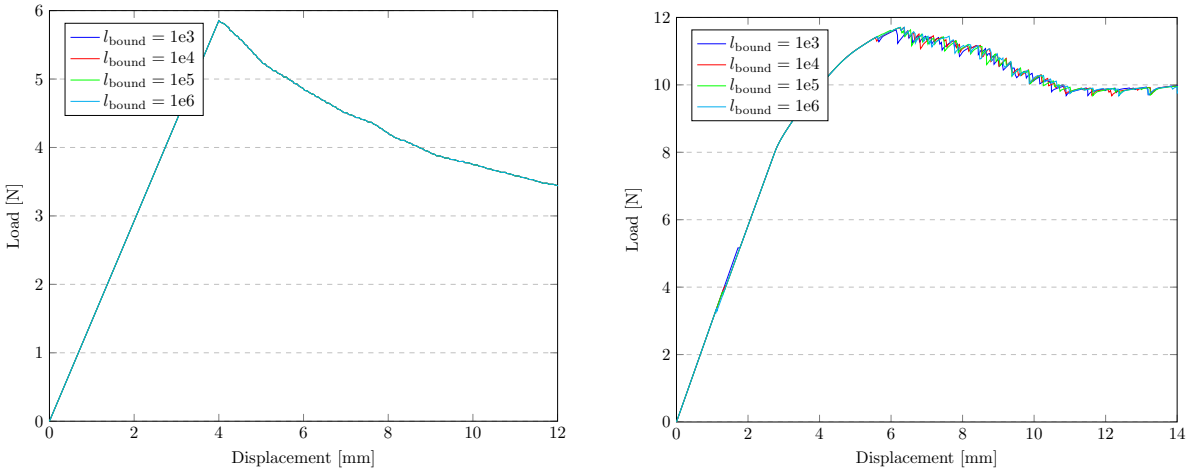

(a) Linear elastic material

(b) Elastic-plastic material

Figure 4.3: Comparison of load-displacement responses of the DCB specimen for a varying lower bound damage l_{bound}

4.2.5. Conclusion

A few conclusions for method 1 can be drawn. Firstly, the interfacial stiffness in the sane material for method 1 will be higher while obtaining the exact same response compared to the current ITLS model. It should be noted that both method 1 and the current ITLS method can adopt an equally high initial interfacial stiffness before this stiffness becomes too high and causes divergence of the numerical model. However, the formulation of method 1 allows us to control the initial stiffness of the undamaged part of the interface by changing the value for l_{bound} without affecting the global response.

The second conclusion follows from the first conclusion and is regarding the influence of initial interfacial stiffness parameter K and the lower bound of the damage function l_{bound}. The simulations with a varying stiffness parameter K have shown that there is a dependency of the model on the parameter K in this method. However, due to the fact that the global response is not influenced by varying values for l_{bound}, this method can be independent of the initial stiffness of the interface. Therefore, the independence is not the expected independence of the model to parameter K but an independence to the parameter l_{bound}. By the addition of l_{bound} the model is capable of acquiring different interfacial stiffness values in the sane material while obtaining similar global responses. It should be noted that in order to accomplish equal results, the value for initial interfacial stiffness K should remain constant for all simulations, which is still a limitation of the model.

Finally, the conclusion can be drawn that method 1 is capable of removing the initial interfacial stiffness dependency in the current ITLS formulation. However, the formulation of method 1 does not allow for simpler calibration of the numerical model, since the same set of parameters needs to be calibrated as for the current ITLS model. Therefore, the only advantage of the method is the possibility to control the interfacial stiffness in the sane material through parameter l_{bound}. It is chosen not to continue this method and to propose a second method that is also capable of simplifying the calibration process.

4.3. Relating damage to the initial interfacial stiffness - Method 2

Method 1, which holds the adaption of the constitutive relations and the boundary conditions of the damage function, proved to be no solution to the problem of the initial stiffness in the ITLS model. Therefore, a new method should be invented that does solve the initial stiffness problem. Chapter 3 showed that there are only two parameters, active in the interface, that have an influence on the global response of the DCB specimen. These parameters are the damage parameter c_1 and the interfacial stiffness parameter K and they are the key pillars to the the second method for the removal of the initial interfacial stiffness dependency.

4.3.1. Adapting the damage function

From Sections 3.2.1 and 3.2.3 it became clear that for an increasing value of parameter c_1 the initial stiffness of the global response decreased and for an increasing value of parameter K the initial stiffness of the global response increased. Method 2 assumes that there is a dependency between parameter c_1 and K that can be used to adapt the definition of the damage function and allows us to obtain the exact same results for simulations with a different value for the input parameter K. The hypothesis is that the influence of an increase in the damage parameter c_1 can be neutralized by an increase of the stiffness parameter K. This would mean that c_1 and K are proportional to each other. The order of the proportionality is investigated by trial and error.

The simulations were executed with the following interfacial parameters, a damage parameter c_3 of 0.01, a length of the damaged zone l_c of 3 mm and an element size of 0.3 mm. After investigation a proportionality between the parameters c_1 and K is found. Fig. 4.4 shows the results for a simulation where the parameters c_1 and K are increased with the same factor, meaning there was a one to one proportionality. For both the LE and EP material a perfect agreement between the responses is obtained. Therefore, the executed simulations give rise to the thought that the parameters c_1 and K are one to one proportional to each other.

This should be investigated further to exclude the possibility that the simulations coincidentally obtained equal results. If one to one proportionality is indeed the solution to the problem of the initial interfacial stiffness dependency, the crack tip location should grow at an equal rate for all variations of the stiffness parameter K. If this crack growth curve shows equal responses, it can be concluded that a solution for the problem is found. Fig. 4.5 shows the crack growth responses for both a LE and EP material. For both materials the curves for a varying stiffness parameter c_1 and K show a perfect resemblance. The curves for the EP material have slight oscillations but the averaged trend of the curves is equal. It can be concluded that one to one proportionality removes any stiffness dependencies in the current ITLS model.

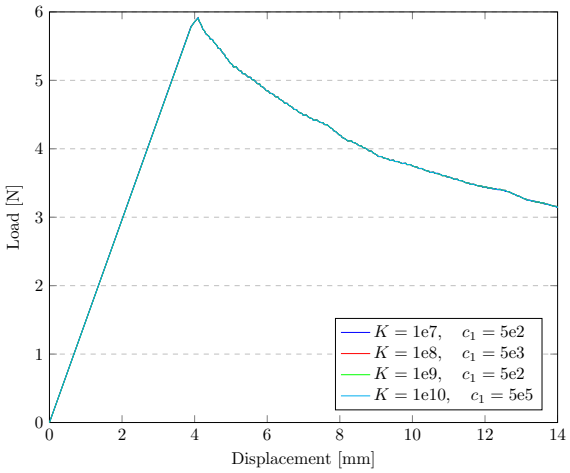

(a) Linear elastic material

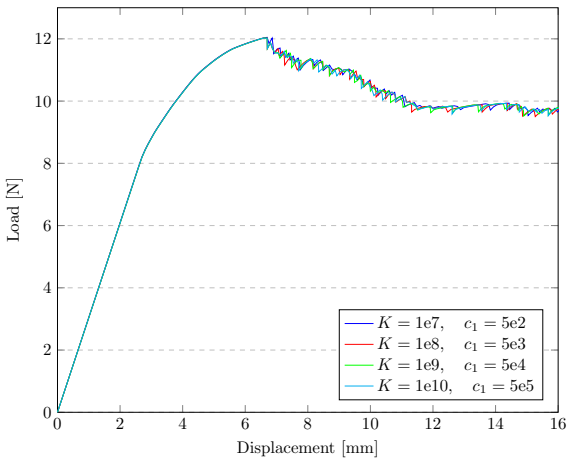

(b) Elastic-plastic material

Figure 4.4: Comparison of load-displacement responses of the DCB specimen with K and c_1 one to one proportional

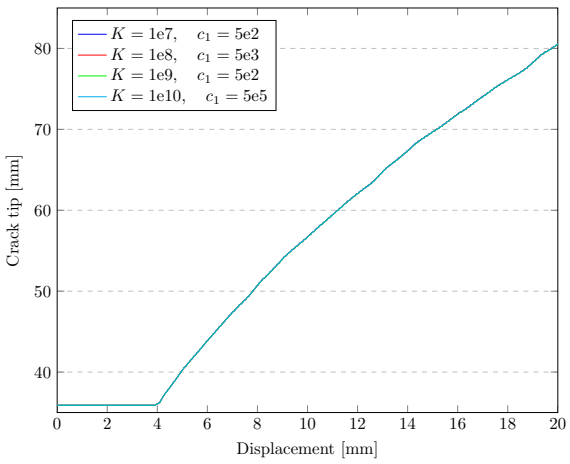

(a) Linear elastic material

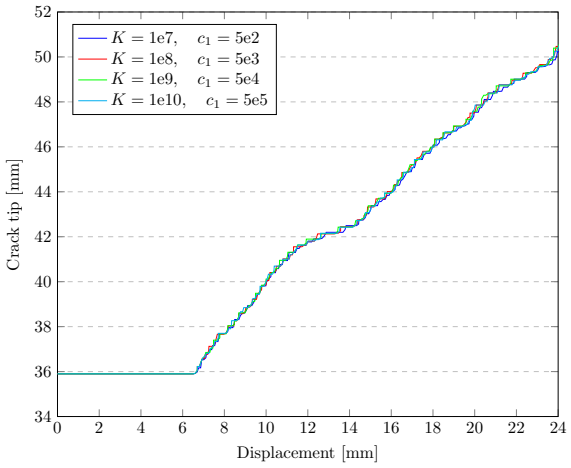

(b) Elastic-plastic material

Figure 4.5: Comparison of crack growth responses of the DCB specimen with K and c_1 one to one proportional

It is clear that a solution for the problem is found. Since proportionality between c_1 and K is proven, the c_1 damage parameter can be replaced such that the numerical model always obtains equal responses independent of the chosen value for the stiffness K. It should be noted that there are certain thresholds and in case these are exceeded, different results for the peak load of the response are obtained. This was already explained in Chapter 3. Therefore, one should always be careful when determining all model parameters and an elaborate parameter calibration should be done before executing simulations to obtain the desired response.

An adaption of the damage parameter c_1 is very straightforward when it is known that parameters c_1 and K are one to one proportional. c_1 can be replaced by a constant parameter multiplied with the stiffness parameter K. This results in the following adapted damage function:

$$d(\phi) = \begin{cases} 0, & \phi \leq 0 \\ c_2 \arctan\left(cK\left(\frac{\phi}{l_c} - c_3\right)\right) + c_4, & 0 < \phi < l_c \\ 1, & \phi \geq l_c \end{cases} \tag{4.9}$$

where parameters c_2 and c_4 are determined as follows:

$$c_2 = \left(\arctan\left(cK\left(1 - c_3\right)\right) - \arctan\left(-cKc_3\right)\right)^{-1} \tag{4.10}$$

$$c_4 = -c_2 \arctan\left(-cKc_3\right) \tag{4.11}$$

In all the expressions c_1 was replaced by cK, where c is a constant with unit mm^3/N that needs to be calibrated. The advantage over the current damage formulation is that only one parameter, the constant c, needs to be calibrated, whereas before both the c_1 and K needed to be calibrated separately. When the constant c is calibrated one can choose a value for parameter K freely. With this new formulation there is no need to manually adjust c_1 and K anymore when one of those two is set to a different value.

4.3.2. Validating proportionality condition

The new found solution for the problem of the ITLS initial interfacial stiffness dependency was only proven with a trial and error based process until this point. There needs to be an explanation for the found proportionality between damage parameter c_1 and initial interfacial stiffness parameter K. To find the explanation the interfacial stiffness over the damaged zone is elaborated. The interfacial stiffness over the damaged zone is given as:

$$K_c = \left(1 - d\right) K \tag{4.12}$$

There are two parts that contribute to the global initial stiffness of the DCB specimen, the initial stiffness of the interface (see Eq. (4.12)) and the stiffness obtained from the bulk material. Since the bulk material remains the same and therefore also its part that contributes to the global initial stiffness, the solution to the global initial stiffness problem relates to the interfacial stiffness over the damaged zone. If somehow for variations of stiffness parameter K this interfacial stiffness can obtain equal results, the initial interfacial stiffness dependency can be removed completely. The interfacial stiffness over the damaged zone is plotted with the use of the new damage formulation to determine if the traction stiffness over the damaged zone can actually explain the similar results in Fig. 4.4 and 4.5.

Fig. 4.6 shows the interfacial stiffness over the damaged zone for a variation of parameter K values. Due to the different values of parameter K there is a difference in interfacial stiffness in the most left part of the graph. However, this difference is accumulated around the crack tip over a very small length of the damaged zone. When looking at the global response of the specimen this difference is negligible. For the remaining part of the damaged zone the interfacial stiffness K_c is equal for varying values of the dummy stiffness K. The equality of the load-displacement responses in Fig. 4.4 and the crack growth curves in Fig. 4.5 is now proven by elaboration of the interfacial stiffness. The interfacial stiffness over the damaged zone can also be elaborated analytically by using a Taylor series around $\phi = l_c$. This proof can be found in Appendix A. For both the numerical and analytical proof a damage parameter c_3 with the value 0.01 is used since this value was also used in the earlier simulations for method 2. It should be noted that the proportionality condition can also be proven numerically and analytically for other values of damage parameter c_3. However, using smaller values for c_3 minimizes the dissimilarity obtained for the interfacial stiffness around the crack tip.

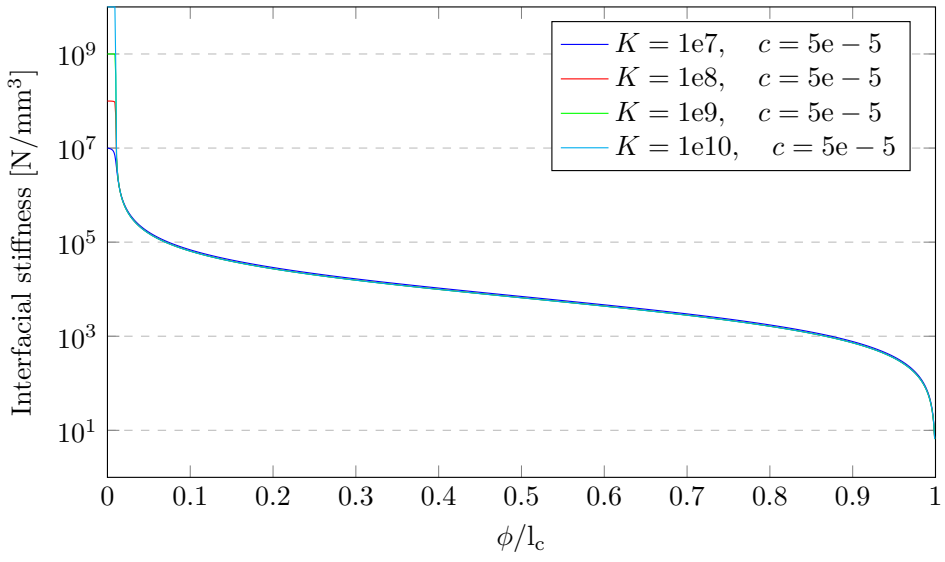

Figure 4.6: Interfacial stiffness over the damaged zone for a varying parameter K and a constant parameter c

To emphasize the difference between this new method for the ITLS and the current ITLS method the traction stiffness over the damaged zone is also plotted with a varying stiffness parameter K and a constant value for the old damage parameter c_1. Here the current formulation for the ITLS is used again to allow us to keep the damage parameter constant without it being scaled by parameter K automatically. Fig. 4.7 shows the results for the traction stiffness over the damaged zone with a constant damage parameter c_1. As expected the results are not equal anymore for the different values of stiffness parameter K. On top of that, all curves in the graph seem to have the same factor difference between the them. This again supports the claim that there is a proportionality condition.

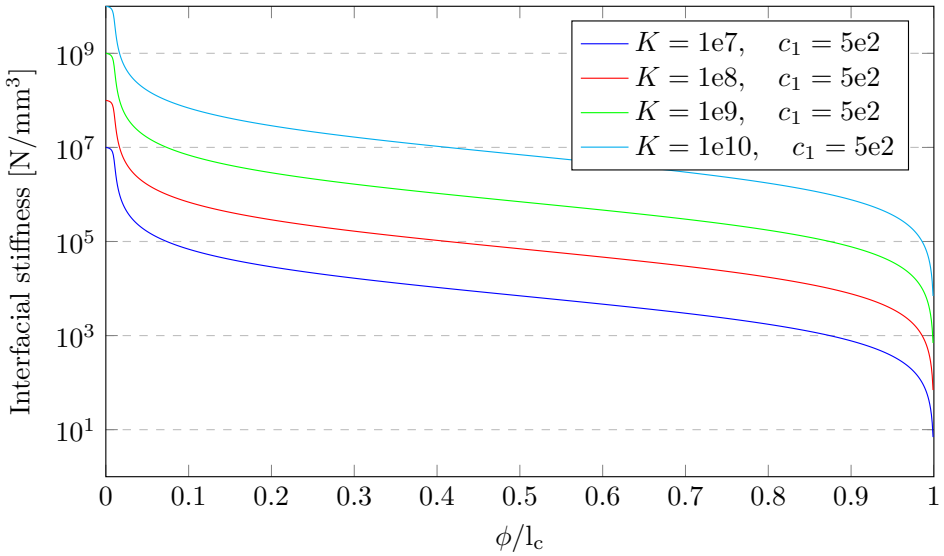

Figure 4.7: Interfacial stiffness over the damaged zone for a varying parameter K and a constant damage parameter c_1

4.3.3. Conclusion

After conducting all simulations a conclusion can be drawn for method 2. The main conclusion that can be drawn is that this new method is able to remove the initial interfacial stiffness dependency in the current ITLS model and thus solves the problem of the current ITLS model. An adaption of the damage formulation was needed to successfully counteract the effects that the parameters c_1 and K had on the global response of the DCB specimen individually. For the remaining part of this research, this adapted ITLS model is used, since it is now known that this model is able to solve the problem for the global initial stiffness. However, there are a few aspects that are not proven yet. It should be proven that the adapted ITLS model will result in accurate responses compared to the CZM and analytical solutions. On top of that, the new model should be validated for other loading types, such as fatigue loading.

4.4. Interfacial stiffness

During the research on the removal of the initial interfacial stiffness dependency, resulting traction curves over the damaged zone from the ITLS model have been found to be remarkable at times. In many simulations the traction had a negative value inside the damaged band near the crack tip. In addition, when the traction was not negative inside the damaged band, a traction profile was obtained with a very high peak that drops at a steep rate which then develops into a plateau that eventually drops to zero if the damage reaches 1. These particular cases occurred several times, Fig. 4.8 shows an example for both cases.

Fig. 4.8a was obtained from a simulation with a LE material and Fig. 4.8b was obtained from a simulation with a EP material. The relevant parameters for the new model are added in the legend, all other interfacial parameters were as described in Section 4.3.1. The obtained shapes for the traction are not as expected when considering the bilinear cohesive traction-separation law. A comparison with a CZM simulation could give more insight in the traction-separation behaviour and might give the reason why traction shapes are obtained that are significantly dissimilar to the bilinear cohesive traction-separation law.

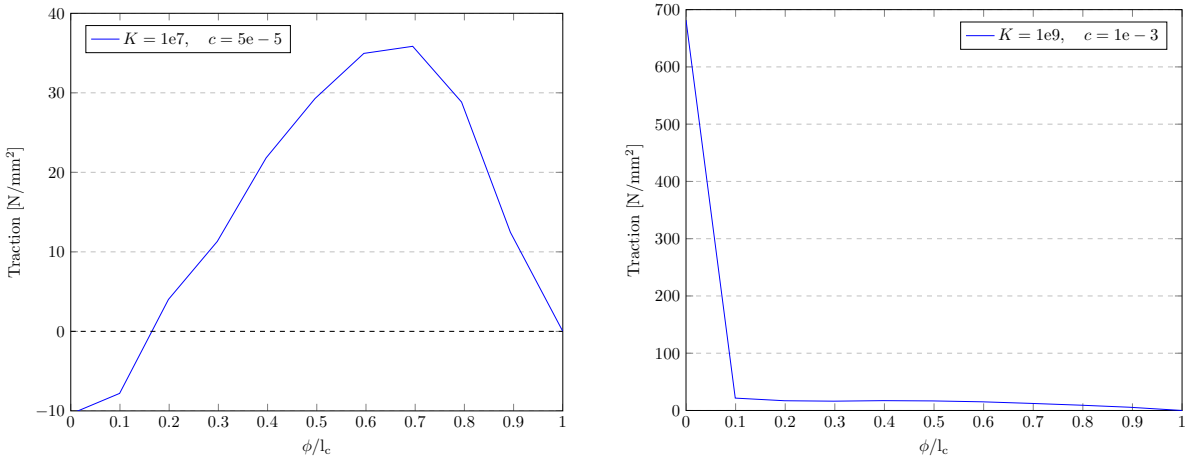

(a) Negative traction

(b) High peak traction

Figure 4.8: Two different traction profiles acquired for ITLS simulations with a DCB specimen

4.4.1. Traction comparison with CZM

To be able to compare the ITLS model with a cohesive model, a CZM model should be defined after which results form the CZM simulation can be obtained and post-processed. The CZM used for this research is taken from the work of Dekker et al. [3] and uses fatigue loading. Therefore, the type of loading differs compared to the quasi-static loading used in this Chapter. However, the main difference originates from the way the crack tip propagates. For quasi-static loading the physical crack tip moves automatically, whereas for fatigue loading the crack tip is pushed forward by the use of an empirical relation, the Paris law. More on fatigue will be discussed in Chapter 5. The difference between fatigue loading and quasi-static loading regarding the damage and subsequently the traction over the damaged zone is negligible. For this reason the CZM with fatigue loading can be compared to the ITLS model. The relevant parameters of this CZM model are depicted in Table 4.1. For this simulation a LE material was used.

Table 4.1: Material properties for the CZM model [3]

E	ν	G_{Ic}	l_c
70.94 GPa	0.33	14.5 N/mm	0.5 mm

In order to understand the difference between the computed traction over the damaged zone both the traction for the ITLS model and the CZM have to be determined with the same parameters. This comparison is shown in Fig. 4.9. It should be noted that damage is determined in a different manner for the CZM. Whereas damage is an input parameter for the ITLS model, the damage in the CZM is a result from the traction-separation relation. For the simulations that were executed in this Section the damage profile for the ITLS model was made to fit the CZM damage in the best possible way.

It becomes clear that there is a significant difference between the two models for the traction distribution over the length of the damaged zone. It should be noted that the traction for the CZM does not decrease to zero inside the damaged band. This is due to the fact that in the used CZM the damage never becomes equal to 1. The obtained traction profile for the CZM shows similarities to a bilinear traction-separation curve. The traction curve for the ITLS model is composed with a numerical model in Matlab. The adapted damage function from section 4.3.1 is implemented. To compute the overall traction for the ITLS model, the dataset for the displacement jumps obtained from the CZM simulation is used. The reasoning behind that is to analyse whether the difference between the traction for the ITLS model and the CZM is based on the computed values for the displacement jumps in the interface or on the shape of the damage function.

Fig. 4.9b shows similar aspects of the traction curve as the traction curve in Fig. 4.8b. The curve from Fig. 4.8b is significantly less smooth but this can be explained by the higher amount of data points in the curves from Fig. 4.9b. Furthermore, the curve from Fig. 4.8b has a lower plateau than the curve from Fig. 4.9b. However, these differences between the two traction curves can be easily explained by the fact that different input parameters were used for both models. The general shape of the traction curve is similar.

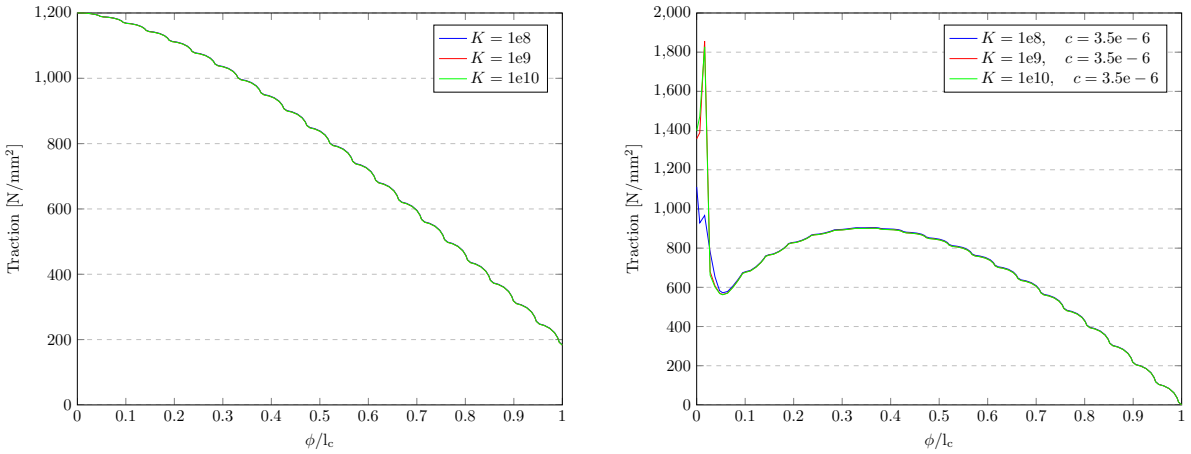

(a) CZM traction

(b) ITLS traction

Figure 4.9: Comparison of traction over the damaged zone for a CZM and ITLS model

This gives reason to believe that in the numerical model used for the ITLS method the computed values for the displacement jumps are similar to the computed displacement jumps in the CZM method. Therefore, the cause for the dissimilarity in the traction over the length of the damaged zone between the two methods should be the shape of the damage profile.

In order to determine if the shape of the damage profile is the actual cause for the difference in traction profiles, the interfacial stiffness over the damaged zone is plotted. This stiffness is computed by Eq. (4.12). Fig. 4.10 shows the interfacial stiffness over the damaged zone for both models with a varying initial interfacial stiffness K. It can be concluded that the interfacial stiffness for the ITLS model can be fitted relatively well to the interfacial stiffness obtained from the CZM analysis. However, it can not take the exact shape.

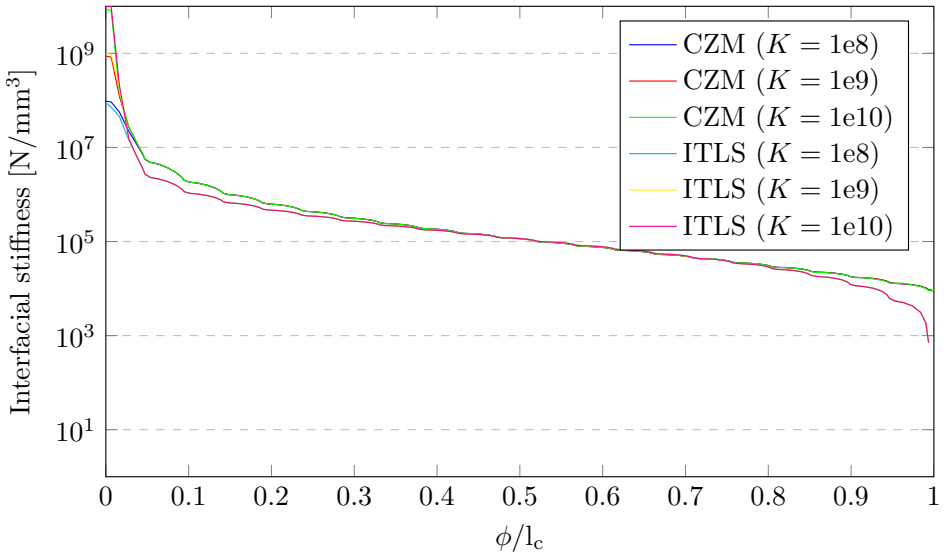

Figure 4.10: Comparison interfacial stiffness over the damaged zone for a CZM and ITLS model

From this figure the difference between the two models seems negligible but the undershoot close to the the crack tip ($\phi/l_c = 0$) for the ITLS model is the cause for the quick drop and subsequently the slight increase in the traction profile in Fig. 4.9b. Therefore, the difference between the ITLS and CZM traction profiles can be explained by the shape of the input damage function in the ITLS model. A possible solution to this could be another type of damage function that can better fit the damage obtained from a CZM analysis. However, this is beyond the scope of this research.

4.4.2. Conclusion

From the results in this Section it is possible to formulate the hypothesis that the shape of the traction profile for the ITLS model is heavily dependent on the chosen damage profile. This would then explain the difference between the ITLS model and CZM model. However, more research should be conducted to fully understand the origin of the acquired traction profiles in the ITLS model. Due to limited time and lower necessity this was not done during this research.

It should be noted that the dissimilarity in the traction profiles does not mean that the acquired traction for the ITLS model is incorrect. This is because it is not proven that the traction profile acquired for the CZM model is the correct traction. Therefore, the only real conclusion that can be drawn is that due to the different damage profiles the acquired traction profile is dissimilar for both methods.

4.5. Results and discussion

Section 4.3 concluded that an adaption of the damage function, which relates the damage function to the numerical initial interfacial stiffness, removes any dependency on the initial stiffness K for the global response. However, this is still purely numerical. To determine if the new method is capable of producing realistic results, the simulations will be compared to analytical results. For the EP material there are no analytical solutions available but the initial stiffness of the specimen should be equal to the initial stiffness resulting from an analytical LE analysis. After all there is no plasticity involved at the start of loading. For the simulations a damage parameter $c_3 = 0.01$ and a length of the damaged zone $lc = 3$ mm are used as input.

The analytical solution for a LE material with crack growth is derived from beam theory following Mi et al. [13]. The linear analytical solution was simply obtained from the load-displacement relationship of a cantilever:

$$P = \frac{3EI\Delta}{2a_0^3} \tag{4.13}$$

where I is the second moment of area of one arm of the cantilever, a_0 is the initial crack length, Δ is the opening displacement and P is load. The decreasing part of the load-displacement relationship is given as follows:

$$\Delta = \frac{2}{3}\frac{\left(WG_cEI\right)^{3/2}}{EIP^2} \tag{4.14}$$

where W is the width of the specimen and G_c is the fracture energy.

Now the analytical solution can be compared to the obtained responses from the adapted ITLS model. Fig. 4.11 shows the comparison between the load-displacement responses for the adapted ITLS model and the analytical model. The LE simulation shows an excellent agreement for the initial stiffness of the DCB re-

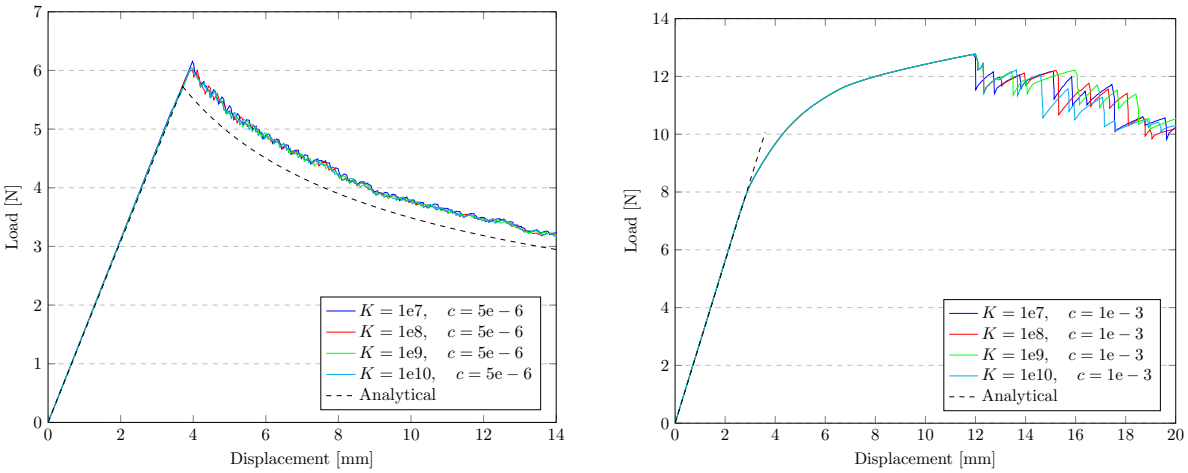

(a) Linear elastic material

(b) Elastic-plastic material

Figure 4.11: Comparison of the load-displacement responses from the adapted ITLS model and from an analytical model

sponse. For the post-peak response there is a slight difference but this is negligible. Overall the the LE simulation shows a good agreement with the analytical solution. The EP simulation shows an excellent agreement

for the initial stiffness of the system as well. Due to the plasticity the response in the plastic region and the crack region can not be compared to analytical models. However, despite the presence of oscillations in the post-peak response the simulations individually show a good agreement to each other.

4.6. Conclusion

In this Chapter, an adaption of the ITLS model is proposed for simulating and propagation in LE and EP materials under quasi-static loading conditions. Two methods for an adaption to the model were discussed. The first option, method 1, proved to be able to remove the interfacial stiffness dependency that was present in the current ITLS by means of the lower bound of the damage function l_{bound}. Similar results were obtained for this method with varying values for l_{bound}. However, this method does not allow for an simpler calibration process. Therefore, the method is not continued in further research.

The second option, method 2, also proved to be able to remove the problem of the interfacial stiffness dependency. Damage parameter c_1 and initial stiffness parameter K were found to be connected to each other, enabling an adaption of the input damage function. By replacing parameter c_1 with a constant multiplied by the initial stiffness (cK) the numerical model no longer suffered from the interfacial stiffness dependency. This simplifies the calibration process, since now only the new constant c has to be calibrated instead of both c_1 and K.

The adapted ITLS model has also proven itself in a comparison with another method to compute the crack response of a specimen. A very good agreement was found between the executed simulations and a numerical model. This proves the accuracy of the adapted ITLS model.

Finally the traction for the adpated ITLS model was investigated and compared to a CZM model. It can be concluded that there are dissimilarities between traction obtained from the ITLS model and the CZM model. Even fitting the input damage function to the damage obtained from the traction-separation law in the CZM does not result in similar traction behaviour. More research should be conducted to be able to conclude whether the traction in the ITLS model is computed in a correct manner. However, this is outside the scope of this research. It should also be noted that it is not possible to demonstrate at this moment if the traction from the ITLS model is incorrect, just as it is not possible to cocnlude that the traction obtained from the CZM model is correct. Both are numerical models with a number of assumptions. Experimental results are needed for a clear answer.

5

Adapted ITLS approach fatigue loading

The goal of this Chapter is to determine whether the adjusted ITLS model following method 2 is capable to deliver an accurate solution for a different specimen and loading type. Therefore, a CT specimen under fatigue loading is investigated. Again plasticity is involved for the simulations, which is very interesting for ductile materials under fatigue loading. Plasticity is assumed to affect the retardation due to crack growth in the specimen. The capability of the adapted ITLS model to capture this retardation is investigated. The specimen will be investigated for both a constant amplitude loading and an overload situation. Finally, conclusions are drawn about the overall performance of the adapted ITLS model to obtain accurate results.

5.1. Paris' law conversion

The previous Chapter presented an adjusted version to the ITLS model created by Latifi et al. [9]. This method 2 using the proportionality condition proved to be a solution to the initial interfacial stiffness dependency in the current ITLS model. The adapted model provides accurate results for a DCB specimen under mode-I quasi-static loading conditions. In order to accept the adapted model as the new approach for crack growth simulations, the model should also be validated for a fatigue loading type. The model must be capable to compute crack growth for all relevant loading types possible in crack growth analysis.

For fatigue analysis in this Chapter a loading envelope approach is used. The maximum load is applied at once, resulting in a constant amplitude (CA) loading. The influence of the cyclic loading is determined by the Paris law (see Eq. (2.19). In most formulations for the Paris law the stress intensity factor (SIF) K_{SIF} is used. However, in this research a formulation containing the variation of energy release rate G is used, because the energy release rate is computed within the numerical framework of the ITLS and can be used directly in the Paris law. Therefore, care should be taken when determining the Paris parameters C and m. These should be converted for G when the parameters are related to a Paris law containing the SIF. In order to convert the parameters C and m a relation between the energy release rate G and the stress intensity factor K_{SIF} is needed:

$$G = \frac{K_{\text{SIF}}^2 \left(1 - \nu^2\right)}{E} \tag{5.1}$$

which is valid for a plane strain model under mode-I loading. This empirical relation is only suitable for linear elastic fracture mechanics (LEFM) as it assumes a singular stress field around the crack tip. In elastic-plastic fracture mechanics (EPFM) stresses are not singular and therefore plasticity influences the crack growth rate at the crack tip. However, there is no relation between G and K_{SIF} known at this moment for fatigue analysis with plasticity involved. Therefore, due to lack of existing relations the LEFM relation is used in this research. It is considered a disadvantage since it infers a less accurate response when plasticity is involved.

Eqs. (5.1) and (2.19) are used to convert the Paris parameters to the correct values when the energy release rate G is used. For simplicity it is assumed throughout this entire Chapter that the fracture energy G_c is equal

to 1, removing it from the Paris law, which gives:

$$\begin{cases} C_{\mathrm{G}} \left(\Delta G\right)^{m_{\mathrm{G}}} & = C_{\mathrm{K}} \left(\left(\frac{\Delta G E}{1-\nu^2} \right)^{\frac{1}{2}} \right)^{m_{\mathrm{K}}} \\ C_{\mathrm{G}} \left(\Delta G\right)^{m_{\mathrm{G}}} & = C_{\mathrm{K}} \left(\frac{E}{1-\nu^2} \right)^{\frac{1}{2} m_{\mathrm{K}}} \left(\Delta G\right)^{\frac{1}{2} m_{\mathrm{K}}} \end{cases} \tag{5.2}$$

From this it follows that the Paris parameters C_{G} and m_{G} relating to the energy release rate G become:

$$\begin{cases} C_{\mathrm{G}} & = C_{\mathrm{K}} \left(\frac{E}{1-\nu^2} \right)^{\frac{1}{2} m_{\mathrm{K}}} \\ m_{\mathrm{G}} & = \frac{1}{2} m_{\mathrm{K}} \end{cases} \tag{5.3}$$

It should be noted that for the simulations that are executed in this research, the relations in Eq. (5.3) were initially used to convert the Paris parameter values related to the SIF to values related to the energy release rate. However, after converting the Paris parameters used by Voormeeren et al. [24], the result was a diverging numerical model. Therefore, the Paris parameter C was adjusted to a value that allowed for converging simulations.

5.2. Input model

The potential of the adapted approach has been evaluated through fatigue analysis of a single test specimen subjected to CA loading. The adapted method is assessed for EP materials through the analysis of a steel compact tension (CT) specimen. The CT specimen is analysed under plane strain conditions.

The geometry and boundary conditions of the CT specimen are shown in Fig. 5.1. In this research the specimen has a width of $W = 100$ mm, a thickness $B = 1$ mm and an initial notch of $a_0 = 31$ mm. The thickness B is equal to 1 mm since this is equivalent to a 2D model. The length of the initial notch is measured from the reference plane, which is positioned through the centerline of the loading pin holes. In the vicinity of the crack large mesh refinements are used to ensure accurate crack growth computation. The elements in this area have a constant mesh size of 0.05 mm.

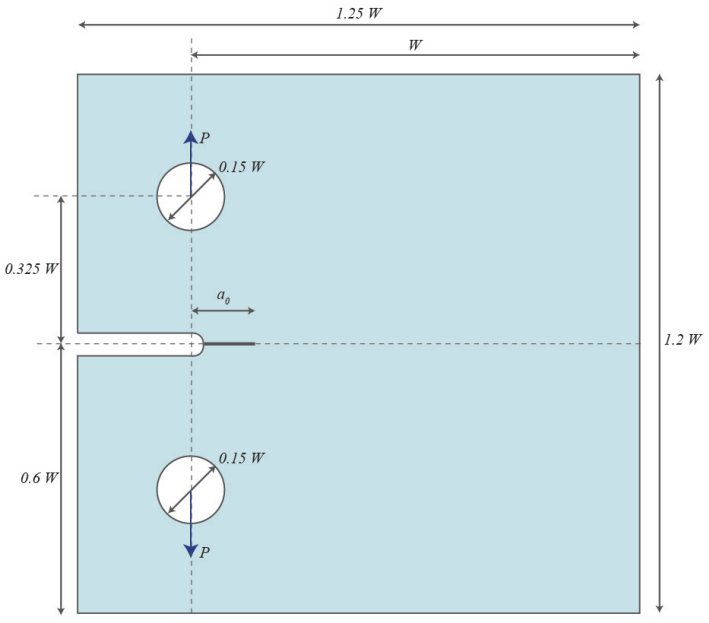

Figure 5.1: 2D CT specimen for simulating crack growth under fatigue loading

A CA load with a stress ratio $R = 0$ is used for all simulations throughout this Chapter for reasons of simplicity. Therefore, there is no difference between the maximum and minimum variation of energy release rate

ΔG. The maximum load applied is varied for different simulations in this Chapter and will be mentioned in the corresponding sections.

As noted in the previous Section, Paris' parameters C and m could be converted from values related to the SIF to values related to the energy release rate. The Paris parameters that were initially used to convert are $C = 3.1 \cdot 10^{-13}$ and $m = 3.75$ [24]. However, divergence occurred when using the converted values according to Eq. (5.3). Therefore, only m was converted, whereas the value for C was found by trial and error in order to obtain a properly converged solution. The final Paris parameters used for all initial simulations are $C = 8.36 \cdot 10^{-6}$ and $m = 1.875$.

The geometry remains constant for all simulations. It is chosen to use an EP material of which the material properties are listed in Table 5.1 according to the material used by Voormeeren et al. [24].

Table 5.1: Material properties for the elastic-plastic material used in fatigue mode-I simulations

E	ν	Q_∞	σ_y^0	b_y	G_{Ic}
210 GPa	0.3	55 MPa	465 MPa	2.38	1 N/mm

5.3. Validating adapted ITLS model

The found initial interfacial stiffness dependency in the current ITLS model under quasi-static loading is present under fatigue loading as well. Voormeeren et al. [24] showed that initial stiffness K affects the number of cycles needed to grow a fatigue crack of certain length. Furthermore, it is assumed that for the current ITLS model the amount of plasticity in the specimen is dependent on the chosen value for the initial interfacial stiffness K. These behavioural aspects of the numerical model are undesirable and should therefore be removed from the model. Since the last Chapter proved that an adapted version of the ITLS model was capable of removing the dependency of the model on the choice for the initial interfacial stiffness K for a specimen under quasi-static loading, it is assumed that the adapted ITLS model will be capable of removing this dependency for a specimen under fatigue loading as well. This needs to be validated in order to investigate whether the adapted ITLS model is an accurate and robust method to simulate fatigue crack growth. At the same time it should be validated whether the adapted ITLS model is capable of obtaining equal amounts of plasticity independent of the initial interfacial stiffness K. In order to validate the adapted model for both aspects, a comparison between the current and the adapted ITLS model is carried out. The comparison enables us in the first place to demonstrate the presence of the two above mentioned issues in the current ITLS model and in the second place to validate the capability of the adapted ITLS model to remove the two issues.

The comparison between both models is carried out for an initial interfacial stiffness range of 1e8 to 1e10 N/mm^3. The damage parameter c_3 had a value of 0, reducing the damage function to the function used by Voormeeren et al. [24]. The length of the damaged zone l_c was chosen as 0.3 mm, resulting in an amount of 6 elements over the damaged zone. The CA loading is equal to 700 N for the current ITLS model and 900 N for the adapted ITLS. The difference in loading is due to numerical robustness of the model. By executing several simulations, it was found that the model is very sensitive to changes in the interfacial parameters c and K and the Paris parameters C and m. These two CA loads enabled both ITLS models to converge to results that could be compared to each other.

5.3.1. Comparison between adapted and current ITLS model

To validate whether the adapted ITLS model is capable of removing the initial interfacial stiffness dependency for fatigue, the variation of energy release rate ΔG versus the crack growth a can be investigated. In order to obtain similar crack growth results for a varying initial interfacial stiffness K, the variation of energy release rate over the growing crack should be equal for all values of K. Furthermore, it should be investigated if the amount of plasticity differs for various values of the initial interfacial stiffness K. This is carried out for both the current and the adapted ITLS model, after which the results can be compared. First the variation of the energy release rate ΔG will be discussed.

VARIATION OF ENERGY RELEASE RATE

Fig. 5.2 shows the variation of energy release rate ΔG over the crack growth for the current and adapted ITLS model. From the figure a few conclusions can be drawn. The results for the current ITLS model are discussed first. The curves show large oscillations, which can be explained by the sensitivity of the numerical model.

During the execution of the simulations the model proved to be very sensitive to the values for parameters C, m and c_1. This made it difficult to find a combination of parameter values capable of executing a simulation that converges for various initial interfacial stiffness values and a constant damage parameter c_1. The oscillations are the largest for $K = 10^8$ N/mm^3, which can be explained by the fact that the damage parameter c_1 is relatively large compared to the initial interfacial stiffness. It was accomplished that besides the one to one proportionality for quasi-static loading a dependency between these two parameters exists. Therefore, the choice for a value of one of the parameters limits the choice for the value of the other parameter regarding the accuracy of the response. Furthermore, the results show that for the different values of parameter K the variation of energy release rate ΔG differs regarding the averaged trend of the oscillations. This gives definitive proof that an initial interfacial stiffness dependency is truly present in the current ITLS model for fatigue.

Secondly, the results for the adapted ITLS model are discussed. Fig. 5.2b shows that for varying values for the initial interfacial stiffness K the variation of energy release rate over the crack growth is similar. This suggests that the computation of the energy release rate in the interface is independent of the value for the initial interfacial stiffness K, which then implies that similar crack growth can be obtained independent of the chosen initial interfacial stiffness. The variation of energy release rate for the simulation with an initial interfacial stiffness of 10^8 N/mm^3 is slightly dissimilar to the results of the other two simulations. The curve has more oscillations and lies below the other two curves. However, these dissimilarities are negligible and it can be concluded that the proportionality condition seems to work for fatigue analysis regarding the dependency on the initial interfacial stiffness. In order to validate the proportionality condition to a larger extent, the amount of plasticity and the size of the plastic zone needs to be checked.

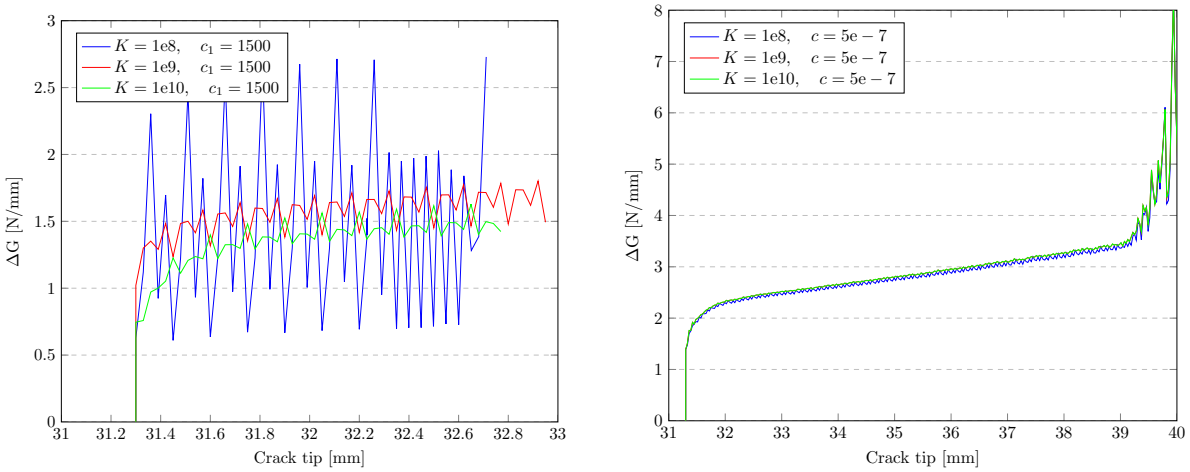

(a) Current ITLS model

(b) Adapted ITLS model

Figure 5.2: Variation of energy release rate ΔG versus crack length a for steel CT specimen

PLASTIC ZONE

It is assumed that the current ITLS model affects the amount of plasticity and the size of the plastic zone around the crack tip. The capability of the adapted ITLS model, and therefore the proportionality condition, to overcome this behaviour is investigated. A model that computes equal plastic strains and subsequently plastic stresses independent of the chosen value for initial interfacial stiffness K is desired. The capability of both the current and the adapted ITLS model to obtain equal plastic zones is investigated by comparing the contour plots of the Von Mises stresses in the CT specimen around the crack tip. From these contour plots the size of the plastic zone can be obtained as well as the values of the stresses.

Fig. 5.3 depicts the Von Mises stress around the crack tip for all simulations with the current ITLS model. All contour plots are taken at a moment where the crack tip location is equal for all simulations. This allows for a comparison of the plastic zone in each simulation. The plots show that the amount of plasticity differs for varying values of the initial interfacial stiffness K. The stresses are not of equal magnitude for the three simulations. Furthermore, the size of the plastic zone is dissimilar when equal crack growth is obtained. This behaviour is undesired, since in reality the results should be independent of numerical parameters such as

the initial interfacial stiffness. This proves that the amount of plasticity in the current ITLS model is dependent on the choice for the initial interfacial stiffness K when fatigue is taken into account.

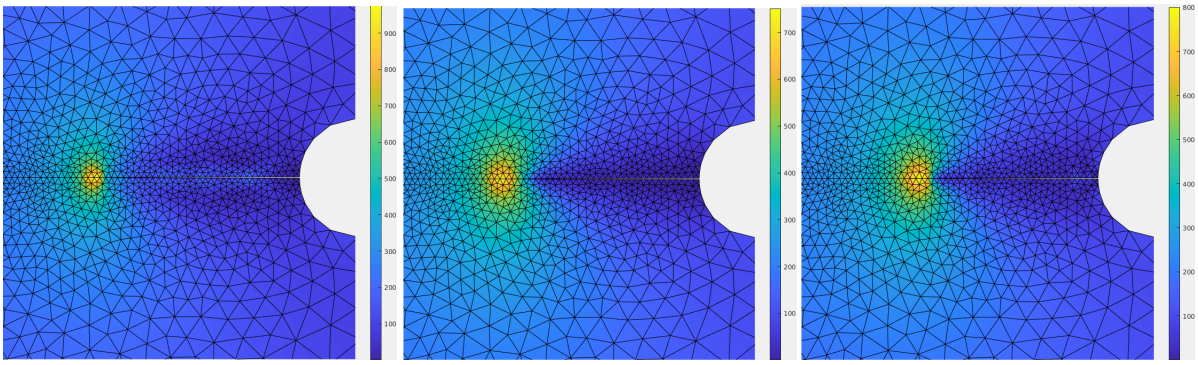

(a) $K = 10^8$ N/mm^3 (b) $K = 10^9$ N/mm^3 (c) $K = 10^{10}$ N/mm^3

Figure 5.3: Contour plot Von Mises stresses along the crack surface for current ITLS model (crack tip has grown from 31 mm to 32.7 mm)

The undesired influence of the initial interfacial stiffness on the amount of plasticity needs to be removed. It is assumed that the adapted ITLS model is capable of achieving this. Therefore, the contour plots for the Von Mises stress are shown for simulations with the adapted ITLS model. Fig. 5.4 depicts the Von Mises stress around the crack tip for the adapted ITLS model. To allow for a good comparison of the plastic zone, the contour plots are taken at a moment where all simulations have obtained an equal crack growth. The contour plots show a good agreement between the three simulations with a varying parameter K. The stresses around the crack tip are higher than the yield stress, which means plasticity is present around the crack. This is of importance since plasticity is needed to validate whether the adapted ITLS model is capable of removing a dependency between the plasticity and stiffness parameter K. The magnitude of the stresses show a good resemblance and the plastic zone is of an equal size in every simulation. This result suggests that the chosen values for the initial interfacial stiffness K do not influence the amount of plasticity anymore.

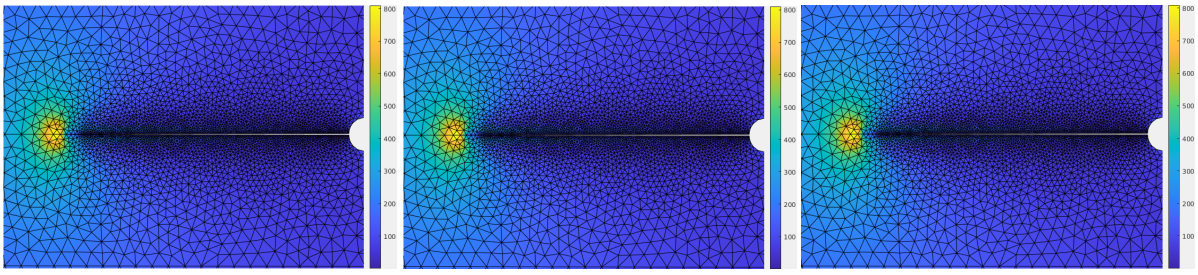

(a) $K = 10^8$ N/mm^3 (b) $K = 10^9$ N/mm^3 (c) $K = 10^{10}$ N/mm^3

Figure 5.4: Contour plot Von Mises stress along the crack surface for adapted ITLS model (crack tip has grown from 31 mm to 40 mm)

CONCLUSION

Conclusions from the comparison between the current and adapted ITLS model can be drawn. Prior to the simulations, it was assumed that the current ITLS model suffered from a dependency on the initial interfacial stiffness for the computation of the crack growth and the plasticity. Furthermore, it was assumed that the adapted ITLS model is capable to overcome these issues. The results in this section support both assumptions, since the current ITLS model obtained dissimilar plastic behaviour and computed values for the variation of energy release rate ΔG, whereas the adapted ITLS obtained similar results for both aspects. The results suggest that the adapted ITLS model has the intended influence for fatigue analysis by removing the undesired dependencies in the current ITLS model. To be able to propose the adapted model as the new approach to crack analysis under fatigue loading, further validation of the model is needed. In a next step, the accuracy of the computation of crack propagation needs to be validated.

5.3.2. Crack growth adapted ITLS

The adapted ITLS model shows great potential for fatigue analysis. However, this needs to be validated further. The next step is to compare the computed crack growth over the amount of cycles. An accurate numerical model should be able to compute the same crack growth rate independent of the initial stiffness given to an interface. Therefore, the simulations for the adapted ITLS model from the previous section are examined further. The crack growth versus the amount of cycles needed to reach that crack growth is investigated to validate whether the previously found similarities between the computed values for the variation of energy release rate for a varying initial interfacial stiffness can be translated directly to crack growth results that are similar as well. The results for the crack growth over the number of cycles are depicted in Fig. 5.5. From the figure it becomes clear that the crack growth for an initial interfacial stiffness of $K = 10^8$ N/mm^3 differs slightly from the other two curves. This can be explained by the results in Fig. 5.2b for the same initial interfacial stiffness variation. The variation of energy release rate for the stiffness $K = 10^8$ N/mm^3 slightly differed from the other two results. There were minor oscillations, suggesting less accuracy, and a slightly lower variation of energy release rate. These dissimilarities are directly translated to the results for the crack growth over the number of cycles in Fig. 5.5. For initial interfacial stiffness 10^9 and 10^{10} N/mm^3 there is a perfect agreement.

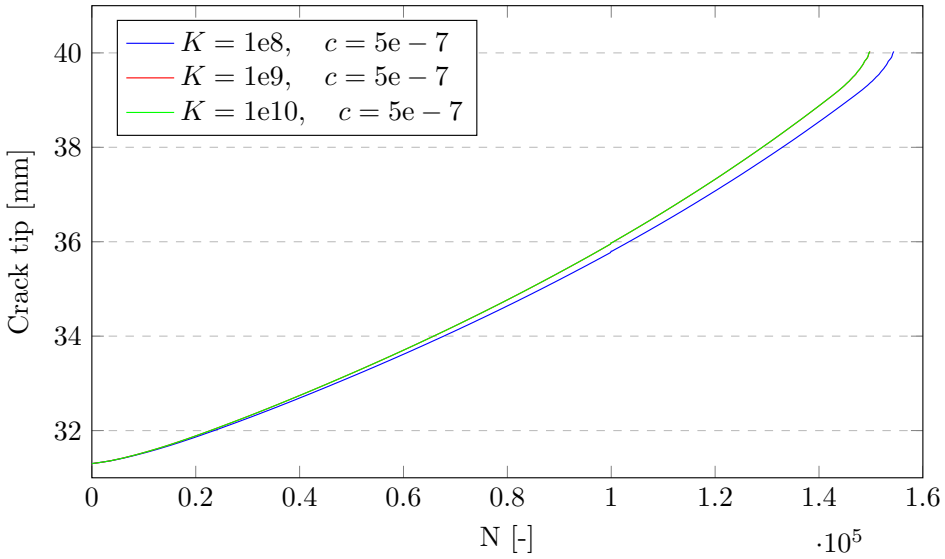

Figure 5.5: The crack growth versus the number of cycles for the adapted ITLS model

In order to overcome this slight dissimilarity an elaborate parameter calibration is needed. However, there is a quick fix for such dissimilarities. The Paris parameters determine the distance over which the crack propagates every time step. Therefore, these parameters, more specifically the C parameter, could be adjusted to obtain a slightly different crack growth. The analytical model for LEFM fatigue crack growth in a CT specimen can then be used to find the value needed for this C parameter. Then a new simulation with the adjusted C parameter can be executed to obtain crack growth over the number of cycles similar to that of the simulations for the other initial interfacial stiffness values.

Analytically the number of cycles required to grow a crack from a_0 to a certain length a_f can be determined by Paris' law (Eq. (2.19)) through simple integration:

$$N = \int_{a_0}^{a_f} \frac{1}{C\Delta G^m} \mathrm{da} \tag{5.4}$$

This can be used to determine the value of parameter C necessary for obtaining the same amount of cycles for all simulations. The variation of energy release rate computed through the simulations are used as input for the analytical expression. From investigation it follows that for the simulation with an initial interfacial stiffness of 10^8 N/mm^3 the Paris parameter C should be equal to $8.62 \cdot 10^{-6}$. When this value is then used in the numerical model for a new simulation the crack growth over the number of cycles as depicted in Fig. 5.6 is obtained. It shows that there is now a perfect resemblance between the results for the three simulations.

Furthermore, it can be concluded that a method is found that can be used to overcome slight differences in fatigue analysis results due to numerical issues. However, when large dissimilarities in the response of the specimen are obtained this post-processing method may not suffice. In that case an entire calibration of the numerical parameter set may be needed. Further research on this should be carried out for better understanding.

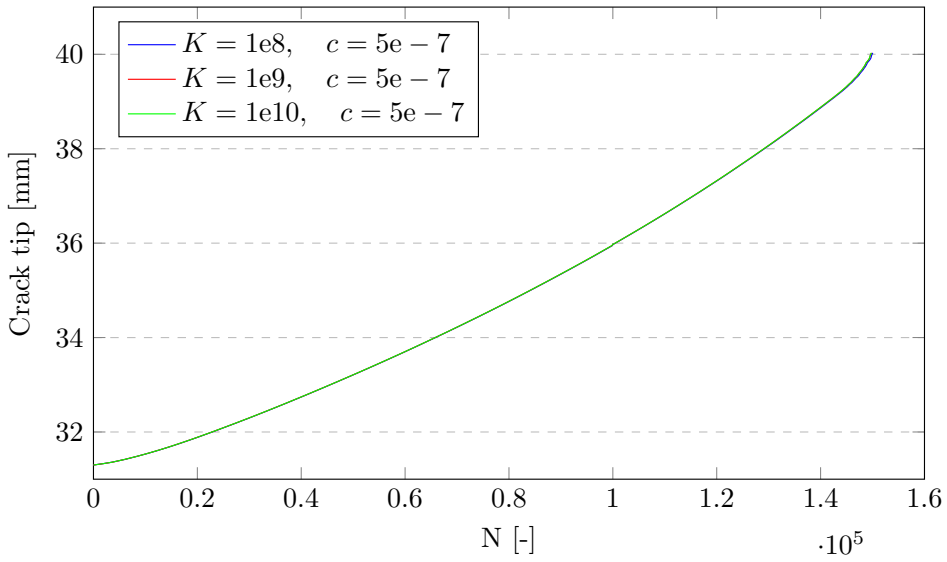

Figure 5.6: The crack growth versus the number of cycles for the adapted ITLS model with calibrated C parameter

5.3.3. Validating proportionality condition with an overload

The last step in this research for the validation of the adapted ITLS model with the proportionality condition is to execute simulations with an overload (OL). The OL affects the amount of plasticity around the crack tip. Generally, an OL incidentally enlarges the plastic zone around the crack tip, resulting in a retardation of crack growth. Due to the influence of the initial interfacial stiffness on plasticity in the current model, simulations with overloads give accuracy issues. However, the adapted ITLS model showed no influence of the initial interfacial stiffness with CA loading and has therefore great potential. Simulations similar to those for the CA loading with the adapted ITLS model are executed to validate this model for fatigue with an OL.

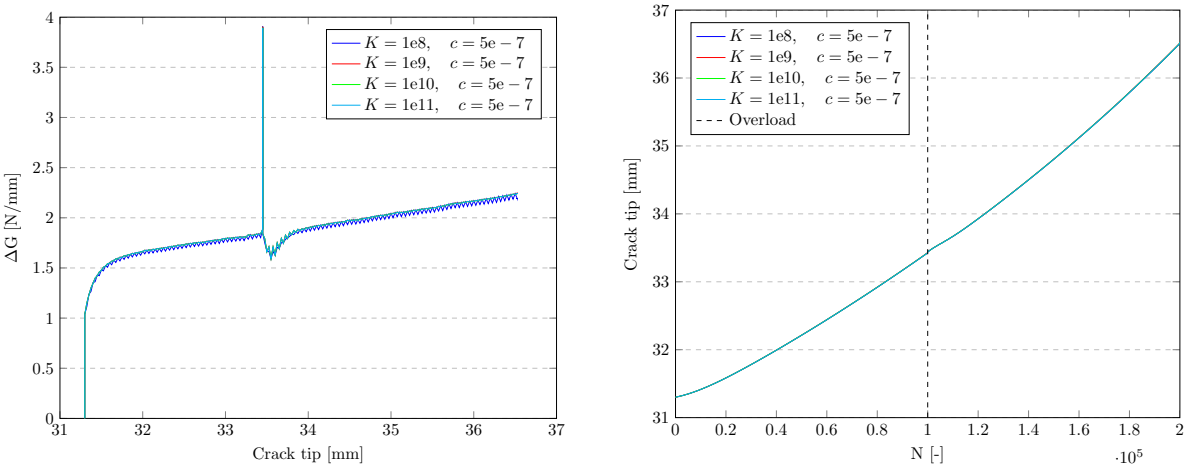

(a) ΔG versus a

(b) a versus N

Figure 5.7: Variation of energy release rate ΔG versus crack length a and The crack length a over the number of cycles needed to reach a

The symmetry for the CT specimen is equal to the symmetry described in Section 5.2. The loading for this analysis consists of a constant part of 750 N and an OL of 1125 N. The length of the damaged zone l_c is

equal to 0.3 mm and the damage parameter c_3 is equal to 0. Both the constant c and the initial interfacial stiffness K remained the same as for the CA loading analysis with the addition of a fourth simulation with an initial interfacial stiffness $K = 10^{11}$ N/mm^3. Fig. 5.7 depicts the results of the simulations with an OL for four different values of the initial interfacial stiffness K. It should be noted that for the initial interfacial stiffness of 10^8 N/mm^3 the analytical method for calibrating the Paris parameter C is used. This method was described in Section 5.3.2. The results for the variation of energy release rate ΔG (see Fig. 5.7a) show a good agreement, where only the results for $K = 10^8$ N/mm^3 is slightly less accurate with some oscillations. However, this inaccuracy could be solved for the obtained curves of the crack growth versus the number of cycles by the use of a calibrated Paris parameter C. In this case the parameter C has a value of $8.5 \cdot 10^{-6}$ for the simulation with $K = 10^8$ N/mm^3 instead of $C = 8.36 \cdot 10^{-6}$ for the other simulations.

The crack growth over the number of cycles shows a perfect agreement between the simulations (see Fig. 5.7b). Even after the OL is applied a perfect agreement is found for the crack growth curves. The results show the potential of the adapted ITLS model to capture accurate and equal responses.

5.4. Conclusion

In this Chapter the capability of the adapted ITLS model with the proportionality condition for simulating crack growth under fatigue loading is discussed. Two types of analysis are discussed, the analysis with CA loading and the analysis with an OL. Both analyses were executed to investigate the capability of the proposed ITLS model to obtain accurate results for crack growth under fatigue loading. A few conclusions can be drawn.

From the results for both the analysis with only CA loading and the analysis with an OL, it can be concluded that the proposed adapted ITLS model is capable of removing the initial interfacial stiffness dependency in the current ITLS model. Furthermore, the amount of plasticity in the model seems to remain constant for a varying initial interfacial stiffness K, whereas this was not the case for the current ITLS model. This makes the model independent of the initial interfacial stiffness in a more general context. However, this is not a full proof that the amount of plasticity remains constant for the different simulations. In order to prove it definitively the equivalent plastic strains should be plotted.

Lastly, it became clear from the results for the current ITLS model and the simulation with $K = 10^8$ N/mm^3 for the adapted ITLS model that the numerical model is sensitive to the parameter input. For the adapted model this minor dissimilarity could be fixed by adjusting the Paris parameter C but further research should be executed to investigate the impact of the parameter input on the computed crack growth over the number of cycles.

6

Conclusions and recommendations

In this thesis the dependency on the choice for the initial interfacial stiffness of the ITLS model is investigated. A method is proposed that is capable of eliminating this dependency. This method is validated for analyses under quasi-static loading conditions and fatigue loading conditions. In Section 6.1 the conclusions are given based on the research objective and research questions as defined in Section 1.3. Section 6.2 presents recommendations for further research.

6.1. Conclusions

To assess the research objective two research questions and three sub-questions were formulated. The research questions and sub-question(s) associated to it are discussed individually:

1 *Is there an initial interfacial stiffness dependency in the current formulation for the interfacial thick level set model?*

Within this thesis a parameter study was conducted with the aim to determine which interfacial parameters are affecting the response of a DCB specimen. Each parameter was varied individually after which the influence on the global response was evaluated. The parameters of interest were: the damage parameters c_1 and c_3, the length of the damaged zone l_c and the initial interfacial stiffness K. The length of the damaged zone proved to be of no influence on the DCB response. This provides the possibility to use a coarser mesh while maintaining the same accuracy. It should be noted that enough elements are present inside the damaged band, otherwise the amount of integration points is too small to capture the correct damage profile resulting in less accuracy. The damage parameter c_3 also has no influence on the global response for the DCB specimen for the lower value range. When the value of c_3 becomes higher or equal to 0.5 there is a slight influence on the global response. However, these higher values for c_3 are used mainly in continuous TLS models, whereas the ITLS model mostly uses low values already, which allows for damage shapes more similar to shapes obtained from cohesive models.

The remaining two parameters both have proven to be of significant influence on the global response of the DCB specimen. It is as expected that the damage parameter c_1 has a significant influence on the response of the specimen. Latifi et al. [9] already showed that the choice for a certain damage function affects the response of a specimen. Since c_3 only results in a minor influence with a value above 0.5, the larger part of the influence of the damage function should be related to the c_1 parameter. It could be concluded that an increasing value for c_1 results in a decreasing initial stiffness of the DCB specimen. However, one should always take care when using a high valued c_1 parameter since this could require mesh refinements or even the use of higher order elements to retain accuracy. The initial interfacial stiffness K is the second parameter that has a significant influence on the specimens behaviour. The simulations showed that for an increasing value of parameter K, the initial stiffness of the DCB response increases as well. It is also demonstrated that there is a certain relation between parameters c_1 and K, which was adopted as one of the solution strategies for answering the second research question in this thesis. The threshold for the combination of the two parameters is dependent on several factors such as used material and geometry. Calibration of these parameters for the used specimen is needed to ensure accurate results and to prevent spurious initiation of damage.

The sub-question to this research question was: *Are the effects significant for both linear elastic and elastic-plastic materials?*. The results showed that the global initial stiffness, peak loads and amount of oscillations were affected similarly for a LE and an EP material due to a varying initial interfacial stiffness K. So it can be concluded that the effects due to the damage parameter c_1 and initial stiffness parameter K are present in both material types. Overall it is concluded that there is an initial interfacial stiffness dependency present in the current ITLS model that needs to be removed.

2 *How can the formulation of the current ITLS model be adapted such that the effects on the global behaviour, resulting from the initial interfacial stiffness, are removed?*

The previous research question has proven that there is an initial interfacial stiffness dependency in the current ITLS model. This stiffness dependency has to be removed such that similar responses can be obtained when using different values for the initial interfacial stiffness K. In order to achieve the desired result, two methods were proposed. The first method was based on the assumption that the solution to the initial stiffness dependency is based on an adaption of the constitutive relations for the interface. Instead of initial interfacial stiffness K, the new expression $\frac{K}{d}$ was used, which included the adaption of the damage boundaries. In this adapted damage definition the damage grows from l_{bound} to 1. After elaborating the method and comparing the required results, this method proved to be capable of resolving the initial interfacial stiffness problem and obtaining similar behaviour as was obtained for the current ITLS model. By adjusting the new parameter l_{bound} the interfacial stiffness of the sane material can be varied without affecting the global response, which is essentially a solution to the initial interfacial stiffness dependency in the current ITLS model. However, the initial interfacial stiffness K should remain constant for all simulations and the parameter calibration process does not become simpler by the use of this method, which is considered to be a limitation of this method. Therefore, a second method was proposed.

The second method was based on the assumption that there is a certain relation between the damage parameter c_1 and the initial interfacial stiffness parameter K. Since increase in both parameters resulted in an opposite influence on the initial stiffness of the DCB specimen, a certain proportionality between c_1 and K seemed to be of importance. Executing simulations on a trial and error basis resulted in a one to one proportionality between parameters c_1 and K. When using this proportionality condition an excellent agreement was found between simulations with a varying value for the initial interfacial stiffness for both LE and EP materials. Moreover, the crack growth rate showed an excellent agreement as well. The proportionality can also simply be explained without looking at the results from simulations. When an interface becomes stiffer the rate at which the damage function grows also has to become higher to overcome the extra numerical stiffness. Otherwise, the damage grows slower resulting in a postponed crack initiation and therefore a higher peak load. However, this is more intuitively than an actual proof. The actual proof was found when the interfacial stiffness $(1-d)K$ over the damaged zone was elaborated numerically and analytically. Since the initial stiffness of the DCB specimen consists of two parts, the stiffness from the bulk and the stiffness from the interface, the solution is found when the stiffness of the interface remains constant for varying initial interfacial stiffness K values. The curves for the simulations with the proportionality condition resulting from the numerical elaboration showed a perfect agreement, whereas the curves without proportionality showed dissimilar results. By using a Taylor series around $\phi = l_c$ to elaborate the interfacial stiffness analytically, the proportionality condition could also be proven. Both the numerical and the analytical elaboration of the interfacial stiffness demonstrate how the proportionality condition removes the initial interfacial stiffness dependency in the ITLS model.

The found proportionality condition enabled a new formulation for the damage inside the ITLS model. With this adapted damage formulation the numerical model becomes independent of the chosen value for the initial interfacial stiffness K. This already answers a part of the first sub-question for this research question, which was: *Is it possible to adapt the formulation such that the renewed ITLS is applicable to both linear elastic and elastic-plastic materials in a quasi-static analysis?*. For a complete answer a comparison between an analytical analysis and the adapted ITLS model needs to be carried out. This comparison was performed to ensure the accuracy of the adapted ITLS model. Again both a LE and an EP material were investigated. Since there is no analytical solution for the EP material, the analytical LE definition is used to obtain the initial stiffness of the linear elastic part of the global response. Subsequently, the responses from the simulations were calibrated to this global initial stiffness. Both the LE and EP material showed a very good agreement with the analytical solution. It was found

that for the LE material the post-peak response shows the exact same averaged trend but it is slightly higher than for the analytical solution. However, this dissimilarity is negligible. For the EP material there was no analytical result to compare the post-peak responses to but there was a perfect agreement between the simulations themselves. Therefore, it can be concluded that the adapted ITLS model is applicable to both LE and EP materials for an analysis under quasi-static loading.

During the research the obtained traction curves over the damaged zone were found to be remarkable. The shape of the curves differs significantly from traction curves traditionally obtained with a CZM model. After investigation of the damage profiles and subsequently the interfacial stiffness in both models, the hypothesis that the shape of the traction profile is heavily dependent on the chosen damage profile is stated.

In order to prove whether the adapted ITLS model can be proposed as the new approach to model crack growth, the last sub-question needs to be answered: *Does the adjusted method result in accurate solutions for different types of specimen and load cases?* Crack growth is a very common failure type in fatigue analysis. Moreover, the formulation of the ITLS model enables a direct link between damage mechanics and fracture mechanics. The Paris law is fracture mechanics based and is used for fatigue analysis with crack growth. Therefore, the adapted ITLS model also needs to be validated for a fatigue analysis. For this research it was chosen to perform a fatigue analysis on a steel compact-tension specimen containing plasticity. In the current ITLS model the chosen value for the initial interfacial stiffness K is assumed to have an influence on the amount of plasticity in the specimen. The hypothesis is that this influence disappears when the ITLS model is no longer dependent on the choice for the initial interfacial stiffness. To prove this a fatigue analysis with constant amplitude loading and with an overload was conducted. Initially, the results for the variation of energy release rate ΔG were compared for both the ITLS model with and without proportionality. The comparison between the current and adapted ITLS model showed that there is an initial interfacial stiffness dependency for the amount of plasticity occurring around the crack tip. The contour plots for the Von Mises stress showed dissimilarities for the current ITLS model, whereas there was a good agreement for the adapted ITLS model. Furthermore, the variation of energy release rate ΔG for the current ITLS model imparted dissimilar results, which demonstrates that the found initial interfacial stiffness dependency in the current ITLS model is also present in the model for fatigue. The adapted ITLS model results for the variation of energy release rate proved that the proportionality condition is accurate for the simulations in this research.

With the knowledge that the proportionality condition is valid for the fatigue simulations with a CT specimen, the results for the crack growth over the number of cycles was obtained for simulations with CA loading and with an OL. For the simulations for both the CA load and the OL with an initial interfacial stiffness $K = 10^8$ N/mm^3 the Paris parameter C had to be adjusted such that similar crack growth over the number of cycles was obtained. This was necessary due to the slight difference in the variation of energy release rate compared to the other simulations. By using the method of adjusting the Paris parameter C through the use of the analytical expression for the number of cycles, the dissimilarity between simulations is removed. Therefore, the obtained results proved that the adapted ITLS model is capable of acquiring similar solutions when various initial interfacial stiffness values are used. However, a post-processing method is needed in some cases to obtain equal crack growth results. Furthermore, the numerical model proved to be sensitive to the parameter input. Therefore, the adapted ITLS model should be investigated further for fatigue loading, which means that no definitive answer, regarding the accuracy and capability of the adapted ITLS model, to this sub-question can be given. However, the proportionality condition shows great potential for acquiring accurate results for crack growth under fatigue loading independent of the choice for the initial interfacial stiffness K.

6.2. Recommendations

For future research the following recommendations are given.

6.2.1. Proportionality condition

FATIGUE
The capability of the adapted ITLS model to capture the behaviour of a CT specimen under fatigue loading was discussed earlier. The preliminary conclusion that the adapted ITLS model is capable of removing any

initial stiffness dependency in the model for fatigue was presented. The results showed that the variation of energy release rate ΔG and the amount of plasticity, visualized by the contour plot of the Von Mises stress, remained constant for varying values of the initial interfacial stiffness K. However, a contour plot of the Von Mises stress to compare the plasticity for different simulations is not the most accurate proof of the independence of the plasticity. Contour plots for the equivalent plastic strains could be investigated to provide more knowledge.

Furthermore, some simulations required a post-processing adjustment of the Paris parameter C to obtain similar results for the crack growth over the number of cycles. Further research is recommended to remove the need for such a post-processing step. Research on the influence of the parameter input, particularly the Paris parameters, of the numerical model and the robustness of the model could help in this removal.

LOADING MODES

This research has proven that for a mode-I quasi-static loading case with a DCB specimen, the damage parameter c_1 and initial stiffness parameter K should be one to one proportional. It was shown that this removes the initial interfacial stiffness dependency in the ITLS model without any loss of accuracy. However, only simulations for a mode-I loading scheme were conducted. Therefore, it is impossible to prove whether the proportionality condition is still valid when a mode-II, mode-III or even mixed mode loading is applied. Further research on simulations under different loading conditions would be needed to validate the adapted ITLS model for all possible quasi-static loading types.

For fatigue loading a similar research could be conducted. Since the adapted ITLS model showed great potential for simulations with mode-I fatigue loading, expanding to different types of loading modes would be a next step in the validation of this adapted ITLS model.

3D MODEL

This research focused on 2D model simulations. The next step would be to extend the adapted ITLS model to a 3D model. 3D modeling extends the system of equations that needs to be solved to compute the energy release rate. Moreover, the local driving force Y has to be averaged over the nodes along the crack front, after which a variational approximation is taken to compute the energy release rate. Research should be conducted to investigate whether the one to one proportionality is still valid in the extended system of equations for the computation of the energy release rate. This could then validate the accuracy of the proportionality condition in 3D models.

6.2.2. Traction

Tractions over the length of the damaged zone are computed through the existing constitutive relations in the ITLS model. It was shown that both the initial interfacial stiffness K and the damage function d affect the computed traction. For this research the traction from the ITLS model was compared to that of a CZM. Moreover, the damage function, which is an input parameter in the ITLS model and a result from the computed tractions and displacement jumps in the CZM simulation, were compared. The values for the initial interfacial stiffness were kept equal between the models, therefore the observed difference is caused by the input damage function for the ITLS model. It is impossible to determine whether the traction obtained in the ITLS model is correct or incorrect, just as it is impossible to determine this for the CZM. The only conclusion that could be drawn was that the current shape of the damage function makes it impossible to obtain similar traction profiles over the length of the damaged zone when comparing the ITLS and CZM models.

For future research it is advised to investigate the traction profile at the crack plane. Since it is impossible to determine how the traction profile should look exactly, an experimental test could be conducted on a DCB specimen. However, the traction at the crack plane can only be obtained in an inverse manner. It can not be measured directly. Strains could be measured after which these strains can be inversely translated to tractions. This would allow for a comparison between the inversely obtained traction and the ITLS model. One would then need to adapt the ITLS model such that it produces a similar traction profile. If this means adjusting the damage function, it should also be investigated how this would affect the found proportionality condition.

A second solution strategy could be to couple the ITLS damage mechanics with the cohesive zone models. Lé et al. [10] already researched the coupling between the TLS and CZM model. It would be interesting to extend this to the ITLS model to investigate the influence it has on the resulting tractions at the crack plane.

A

Analytical solution proportionality

In Chapter 4 the proportionality condition for the ITLS model was proven numerically. However, this can also be proven analytically by elaborating the interfacial stiffness $(1-d)K$. In order to obtain similar results this stiffness should remain constant for varying values of initial interfacial stiffness K. To obtain this result, the part $(1-d)$ should change with an equal but opposite factor to K. Therefore, the first step is to elaborate the damage definition as proposed for the proportionality condition.

$$d(\phi) = c_2 \arctan\left(cK\left(\frac{\phi}{l_c} - c_3\right)\right) + c_4 \tag{A.1}$$

Where parameters c_2 and c_4 are:

$$c_2 = \left(\arctan\left(cK\left(1-c_3\right)\right) - \arctan\left(-cKc_3\right)\right)^{-1} \tag{A.2}$$

$$c_4 = -c_2 \arctan\left(-cKc_3\right) \tag{A.3}$$

This results in a damage function as follows:

$$d(\phi) = \frac{\arctan\left(cK\left(\frac{\phi}{l_c} - c_3\right)\right) - \arctan\left(-cKc_3\right)}{\arctan\left(cK\left(1-c_3\right)\right) - \arctan\left(-cKc_3\right)} \tag{A.4}$$

This form of the damage function is difficult to elaborate analytically for the investigation of the influence of a varying initial interfacial stiffness K. To be able to elaborate this analytically the Taylor series of this damage function should be used. A Taylor series around $\phi = l_c$ will enable the comparison between the damage resulting from different values for parameter K. The Taylor series of a simple arc-tangent function is given as:

$$\arctan(x) = \begin{cases} \sum_{n=0}^{\infty} (-1)^n \frac{x^{2n+1}}{2n+1}, & -1 \le x \le 1 \\ \frac{\pi}{2} - \sum_{n=0}^{\infty} (-1)^n \frac{1}{(2n+1)x^{2n+1}}, & x \ge 1 \\ -\frac{\pi}{2} - \sum_{n=0}^{\infty} (-1)^n \frac{1}{(2n+1)x^{2n+1}}, & x \le 1 \end{cases} \tag{A.5}$$

Now that the point of expansion and the shape of the Taylor expression is known, the Taylor series for this particular damage function is carried out. It should be noted that it is assumed that an expansion order of

$O(4)$ is sufficient for the proof of the proportionality condition. The result of the expansion is:

$$\begin{aligned} d(\phi) = 1 &+ \frac{cK\left(\phi - l_c\right)}{\left(\arctan\left(cK\left(1-c_3\right)\right) + \arctan\left(cKc_3\right)\right)\left(1 + c^2K^2\left(1-c_3\right)^2\right) l_c} \\ &- \frac{c^3K^3\left(1-c_3\right)\left(\phi - l_c\right)^2}{\left(\arctan\left(cK\left(1-c_3\right)\right) + \arctan\left(cKc_3\right)\right)\left(1 + c^2K^2\left(1-c_3\right)^2\right)^2 l_c^2} \\ &+ \frac{c^3K^3\left(c^2K^2\left(1-c_3\right)^2 - \frac{1}{3}\right)\left(\phi - l_c\right)^3}{\left(\arctan\left(cK\left(1-c_3\right)\right) + \arctan\left(cKc_3\right)\right)\left(1 + c^2K^2\left(1-c_3\right)^2\right)^3 l_c^3} \\ &+ O\left(\left(\phi - l_c\right)^4\right) \end{aligned} \tag{A.6}$$

Then for the part $\left(1-d\right)$ of the interfacial stiffness this results in:

$$\begin{aligned} \left(1-d\right) = &\frac{cK\left(\phi - l_c\right)}{\left(\arctan\left(cK\left(1-c_3\right)\right) + \arctan\left(cKc_3\right)\right)\left(1 + c^2K^2\left(1-c_3\right)^2\right) l_c} \\ &- \frac{c^3K^3\left(1-c_3\right)\left(\phi - l_c\right)^2}{\left(\arctan\left(cK\left(1-c_3\right)\right) + \arctan\left(cKc_3\right)\right)\left(1 + c^2K^2\left(1-c_3\right)^2\right)^2 l_c^2} \\ &+ \frac{c^3K^3\left(c^2K^2\left(1-c_3\right)^2 - \frac{1}{3}\right)\left(\phi - l_c\right)^3}{\left(\arctan\left(cK\left(1-c_3\right)\right) + \arctan\left(cKc_3\right)\right)\left(1 + c^2K^2\left(1-c_3\right)^2\right)^3 l_c^3} \\ &+ O\left(\left(\phi - l_c\right)^4\right) \end{aligned} \tag{A.7}$$

To check the proportionality condition the expression in Eq. (A.7) can be elaborated for two different values of parameter K for any given coordinate ϕ. To be able to express the difference in a percentage, some values are assumed for the different parameters present in the expression. These values are listed in Table A.1. K_1 and K_2 are the two different values for the initial interfacial stiffness used to prove proportionality. Elaboration of the Taylor expansion yields:

Table A.1: Interface properties

c	c_3	K_1	K_2
$5 \cdot 10^{-5}$ mm^3/N	0.01	10^8 N/mm^3	10^9 N/mm^3

$$\left(1-d_{1,2}\right) = \begin{cases} 6.603 \cdot 10^{-5}\left(-\frac{(\phi - l_c)}{l_c} + \frac{(\phi - l_c)^2}{l_c^2} - \frac{(\phi - l_c)^3}{l_c^3}\right) + O\left(\left(\phi - l_c\right)^4\right) & \text{for} \quad K_1 \\ 6.565 \cdot 10^{-6}\left(-\frac{(\phi - l_c)}{l_c} + \frac{(\phi - l_c)^2}{l_c^2} - \frac{(\phi - l_c)^3}{l_c^3}\right) + O\left(\left(\phi - l_c\right)^4\right) & \text{for} \quad K_2 \end{cases} \tag{A.8}$$

From Eq. (A.8) it becomes clear that for K_2 the value of $\left(1-d\right)$ is $\frac{6.603 \cdot 10^{-5}}{6.565 \cdot 10^{-6}} = 10.06$ times lower than the same value for K_1. Opposite to this the value for initial interfacial stiffness K_2 is 10 times larger than that of K_1. Therefore, both effects will neutralize each other, which is shown as follows:

$$\begin{aligned} K_2 &= 10 \cdot K_1 \\ \left(1-d_2\right) &= \frac{6.565 \cdot 10^{-6}}{6.603 \cdot 10^{-5}}\left(1-d_1\right) \approx 0.1\left(1-d_1\right) \end{aligned} \tag{A.9}$$

When this is used to compare the interfacial stiffness $\left(1-d\right)K$ for the K_1 and K_2, the definitive analytical proof is found:

$$\begin{aligned} \left(1-d_1\right)K_1 &= \left(1-d_2\right)K_2 \\ &= 0.1\left(1-d_1\right)10 \cdot K_1 \\ &= \left(1-d_1\right)K_1 \end{aligned} \tag{A.10}$$

Bibliography

[1] M. L. Benzeggagh and M. Kenane. Measurement of mixed-mode delamination fracture toughness of unidirectional glass/epoxy composites with mixed-mode bending apparatus. *Composites Science and Technology*, 56(4):439–449, 1996.

[2] P. E. Bernard, N. Moës, and N. Chevaugeon. Damage growth modeling using the Thick Level Set (TLS) approach: Efficient discretization for quasi-static loadings. *Computer Methods in Applied Mechanics and Engineering*, 233-236:11–27, 2012.

[3] R. Dekker, F. P. van der Meer, J. Maljaars, and L. J. Sluys. A cohesive XFEM model for simulating fatigue crack growth under mixed-mode loading and overloading. *International Journal for Numerical Methods in Engineering*, 118(10):561–577, 2019. ISSN 10970207.

[4] D. S. Dugdale. Yielding of steel sheets containing slits. *Journal of the Mechanics and Physics of Solids*, 8 (2):100–104, 1960.

[5] W Elber. Fatigue Crack Closure Under Cyclic Tension. *Engineering Fracture Mechanics*, 2(1):37–44, 1970.

[6] A. Hillerborg, M. Modéer, and P. E. Petersson. Analysis of crack formation and crack growth in concrete by means of fracture mechanics and finite elements. *Cement and Concrete Research*, 6(6):773–781, 1976. ISSN 00088846.

[7] M. Latifi, F. P. Van Der Meer, and L. J. Sluys. A level set model for simulating fatigue-driven delamination in composites. *International Journal of Fatigue*, 80:434–442, 2015.

[8] M. Latifi, F. P. van der Meer, and L. J. Sluys. Fatigue modeling in composites with the thick level set interface method. *Composites Part A: Applied Science and Manufacturing*, 101:72–80, 2017.

[9] M. Latifi, F. P. van der Meer, and L. J. Sluys. An interface thick level set model for simulating delamination in composites. *International Journal for Numerical Methods in Engineering*, 111(4):303–324, 2017.

[10] Benoît Lé, Nicolas Moës, and Grégory Legrain. Coupling damage and cohesive zone models with the Thick Level Set approach to fracture. *Engineering Fracture Mechanics*, 193:214–247, 2018. ISSN 00137944.

[11] Jean Lemaitre and Jean-Louis Chaboche. *Mechanics of solid materials*. Cambridge University Press, Cambridge, 1990.

[12] Y. Liu, F. P. van der Meer, and L. J. Sluys. Cohesive zone and interfacial thick level set modeling of the dynamic double cantilever beam test of composite laminate. *Theoretical and Applied Fracture Mechanics*, 96(July):617–630, 2018.

[13] Y Mi, M.A Crisfield, and G.A.O Davies. 15. Mi.pdf. *Journal of Composite Materials*, 32(14):1246–1272, 1998.

[14] N. Moës, C. Stolz, P. E. Bernard, and N. Chevaugeon. A level set based model for damage growth: The thick level set approach. *International Journal for Numerical Methods in Engineering*, 86(3):358–380, 2011. ISSN 10970207.

[15] L. A.T. Mororó and F. P. van der Meer. Combining the thick level set method with plasticity. *European Journal of Mechanics, A/Solids*, 79, 2020.

[16] O. Nguyen, E. A. Repetto, M. Ortiz, and R. A. Radovitzky. A cohesive model of fatigue crack growth. *International Journal of Fracture*, 110(4):351–369, 2001.

[17] K. L. Roe and T. Siegmund. An irreversible cohesive zone model for interface fatigue crack growth simulation. *Engineering Fracture Mechanics*, 70(2):209–232, 2003. ISSN 00137944.

[18] J. C.J. Schellekens and R. De Borst. Free edge delamination in carbon-epoxy laminates: a novel numerical/experimental approach. *Composite Structures*, 28(4):357–373, 1994. ISSN 02638223.

[19] A. Turon, J. Costa, P. P. Camanho, and C. G. Dávila. Simulation of delamination in composites under high-cycle fatigue. *Composites Part A: Applied Science and Manufacturing*, 38(11):2270–2282, 2007. ISSN 1359835X. doi: 10.1016/j.compositesa.2006.11.009.

[20] A. Turon, C. G. Dávila, P. P. Camanho, and J. Costa. An engineering solution for mesh size effects in the simulation of delamination using cohesive zone models. *Engineering Fracture Mechanics*, 74(10): 1665–1682, 2007.

[21] Ani Ural, Venkat R. Krishnan, and Katerina D. Papoulia. A cohesive zone model for fatigue crack growth allowing for crack retardation. *International Journal of Solids and Structures*, 46(11-12):2453–2462, 2009.

[22] F. P. van der Meer and L. J. Sluys. The Thick Level Set method: Sliding deformations and damage initiation. *Computer Methods in Applied Mechanics and Engineering*, 285:64–82, 2015.

[23] F. P. Van der Meer, N. Moës, and L. J. Sluys. A level set model for delamination - Modeling crack growth without cohesive zone or stress singularity. *Engineering Fracture Mechanics*, 79:191–212, 2012.

[24] L. O. Voormeeren, F. P. van der Meer, J. Maljaars, and L. J. Sluys. A new method for fatigue life prediction based on the Thick Level Set approach. *Engineering Fracture Mechanics*, 182:449–466, 2017.